LUND UNIVERSITY

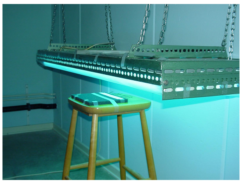

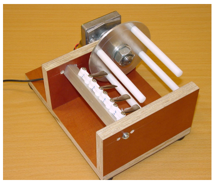

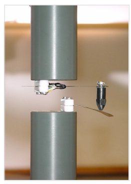

MECHANICAL PROPERTIES OF BIRD FEATHERS
- Influence of UV-Radiation and Mechanical Fatigue

JOHAN BORGUDD

Structural Mechanics

Master's Dissertation

Structural Mechanics

ISRN LUTVDG/TVSM--03/5121--SE (1-70)
ISSN 0281-6679

MECHANICAL PROPERTIES OF BIRD FEATHERS - Influence of UV-Radiation and Mechanical Fatigue

Master's Dissertation by

JOHAN BORGUDD

Supervisors:

KENT PERSSON and GÖRAN SANDBERG,
Div. of Structural Mechanics

THOMAS WEBER and ANDERS HEDENSTRÖM,
Dept. of Animal Ecology

Printed by KFS I Lund AB, Lund, Sweden, April 2003.

For information, address:
Division of Structural Mechanics, LTH, Lund University, Box 118, SE-221 00 Lund, Sweden.
Homepage: http://www.byggmek.lth.se

Acknowledgements

This master thesis work was carried out during the autumn 2002 and winter 2003 at the Division of Structural Mechanics in cooperation with the Department of Animal Ecology and the Department of Cell and Organism Biology, Lund University, Sweden.

Since this interdisciplinary thesis work was evolved during six months, I have to thank all my supervisors for their support.

Thanks to PhD Kent Persson and Professor Göran Sandberg at the Division of Structural Mechanics. Especially Kent who helped me with the mechanical aspects of the work, always taking his time for my questions and worries.

I would also like to thank PhD Thomas Weber and PhD Anders Hedenström who helped me with the ecological aspects of the work. Thanks to Professor emeritus Lars Olof Björn who helped me with the UV-experiment. A special thanks to Technician Thord Lundgren who built the two-point bending test equipment and the mechanical wear equipment and Graphics Technician Bo Zadig who helped me with the layout.

Finally, I would like to thank Emma for her love and support.

Lund, March 2003

Johan Borgudd

Abstract

When birds move around in their natural environment the feathers on the wings are exposed to various factors that reduce their performance, such as UV-radiation, mechanical wearing and bacteria. In time the feathers get worn out and are replaced. This usually happens once a year by a process called moult. Some bird species differs from this pattern and moult twice a year. This behavior may have influence on the mechanical properties of the feathers, and the feathers may respond differently to different kinds of exposure such as UV-radiation and mechanical wearing.

Three experiments were performed on feathers from two different moulting bird species. A UV-radiation-, mechanical wear- and a combination of the two on the Chiffchaff *Phylloscopus collybita*, which moult once a year, and the Willow Warbler *Phylloscopus trochilus*, which moult twice a year. To investigate the influence of these experiments on the mechanical properties of feathers a bending stiffness test was performed after each exposure.

A finite element study was made to investigate the basic mechanical behavior of the feather shaft. A comparison between the FE-simulation and the experiment showed a good agreement.

The results from the experiments showed that for shorter exposure times of UV-radiation the bending stiffness increases then to decrease below the original stiffness value for longer UV-exposures. The mechanical wearing was found to constantly decrease the bending stiffness.

The conclusions from the experiments are that differences between the two bird species exist. From the UV-experiment very small differences in bending stiffness were found. From the mechanical wear-experiment and the mechanical wear part from the combined experiment, larger differences were found, in which the bending stiffness decreases more rapidly for the Willow Warbler than for the Chiffchaff. In the combined experiment the UV-radiation did not increase the bending stiffness as was observed in the single UV-experiment. The combined experiment also made the bending stiffness to decrease more rapidly for the mechanical wearing than was observed in the single mechanical wear-experiment.

Keywords: Feathers, moult, bending stiffness, UV, wear, FEM.

Sammanfattning

När fåglar förflyttar sig i sin naturliga omgivning blir fjädrarna på vingarna utsatta för olika exponering som reducerar deras förmåga såsom UV-strålning, mekanisk utmattning och bakterier. Till slut blir fjädrarna så slitna att de måste bytas ut. Detta sker en gång om året för de flesta fågelarter av en process kallad ruggning. Några fågelarter skiljer sig från detta mönster och ruggar två gånger per år. Detta beteende kan inverka på fjädrarnas mekaniska egenskaper, och fjädrarna kan reagera olika på olika exponering såsom UV-strålning och mekanisk utmattning.

Tre experiment utfördes på fjädrar från två olikruggande fågelarter. Ett UV-strålningsexperiment, mekanisk utmattningsexperiment och en kombination av de två på Gransångaren *Phylloscopus collybita*, som ruggar en gång per år, och Lövsångaren *Phylloscopus trochilus*, som ruggar två gånger per år. För att se om dessa experiment hade någon inverkan på de mekaniska egenskaperna så utfördes ett två punkts böjprov efter varje exponering.

En finita element analys gjordes också för att undersöka de grundläggande mekaniska egenskaperna hos fjäderskaften. En jämförelse mellan FE-simuleringen av böjprovet och det praktiska böjprovet visade god överenstämmelse för böjstyvheterna.

Resultaten från experimenten visade att för kortare exponering av UV-strålning ökade böjstyvheten men för längre UV-exponering minskade den under ursprungsvärdet. Den mekaniska utmattningen minskade konsekvent böjstyvheten med tiden.

Slutsatserna från experimenten är att skillnader mellan de två fågelarterna existerar. Från UV-experimentet hittades bara små skillnader i böjstyvhet men från det mekaniska utmattningsexperimentet och den mekaniska utmattningsdelen av det kombinerade experimentet hittades större skillnader. Där minskade böjstyvheten snabbare för Lövsångaren än för Gransångaren. I det kombinerade experimentet så gjorde inte UV-strålningen så att böjstyvheten ökade som var fallet i det ensamma UV-experimentet. Det kombinerade experimentet gjorde också att böjstyvheten minskade snabbare för den mekaniska utmattningen än i det ensamma mekaniska utmattningsexperimentet.

Contents

Chapter 1

Introduction

1.1 Background

When birds fly, the feathers on the wings are subjected to various exposures, such as turbulence in the air, UV-radiation, bacteria and collisions with branches. In time the feathers get worn out and they need to be replaced. This usually happens once a year by a process called moult. In migratory birds, moult usually takes place after breeding while still on the summer breeding grounds, or moult is postponed until after autumn migration when the bird is in the wintering area. Whether moult takes place in summer or winter is species or population specific. In some rare cases the flight feather moult is divided between the seasons so that part of the flight feathers are moulted in summer and the remaining feathers are moulted in the winter. A few species have a biannual moult and moult the flight feathers completely twice a year [1]. A question arises why the bird that moult twice a year invest in two sets of feathers instead of moulting once a year like most bird species do?

1.2 Objectives

The main objective in this work was to determine the basic mechanical properties of the flight feathers of two differently moulting bird species, the Chiffchaff *Phylloscopus collybita*, which moult once a year after breeding and the Willow Warbler *Phylloscopus trochilus*, which moult twice a year. The work was divided into two subtasks:

- An experimental study of the influence of exposures of UV-radiation and mechanical wearing on the bending stiffness of feathers as well as a comparison between the two bird species, i.e. if the moult frequency has any impact on the measured mechanical properties.

- A numerical study of the basic mechanical behavior of the feather shaft by aid of the finite element method.

1.3 Bird species

1.3.1 General remarks

The Chiffchaff and the Willow Warbler are very similar birds as evident from figure 1.1, and are easiest separated by their singing. The wing length of the Chiffchaff is about 10 *mm* shorter than the Willow Warbler and the feathers on the wings are about 5 *mm* shorter. However, they differ in migratory habits such that the Willow Warbler migrates to tropical and southern Africa for wintering, while the Chiffchaff migrates to the Sahel region just south of the Sahara.

Figure 1.1: *The Chiffchaff and the Willow Warbler [2].*

1.3.2 Chiffchaff

The Chiffchaff is a common bird in Sweden with approximately 5 million nesting pairs. It has its name because of how it sounds when it sings. It moults in August while still residing in Sweden but moves to the north of Africa during the winter.

1.3.3 Willow Warbler

The Willow Warbler is the most common bird in Sweden with approximately 15 million nesting pairs. A special character with this species is that it has a biannual moult. It replaces its feathers twice a year; a first moult after termination of breeding in the summer and a second moult during the winter when in Africa.

Chapter 2

Properties of feathers

2.1 General remarks

Feathers are one of the most complex integuments among the vertebrate animals. Their many parts display an enormous variety of modifications. For example can the longest feather be up to 1000 times longer than the shortest. Feathers are composed of about 91 % protein, 8 % water and 1 % lipids. The type of protein is called keratin, a sulfur containing, colorless, fibrous protein. It is the structure of keratin that gives the feather its strength and flexibility.

There are five categories that represent the main structural types of feathers: 1) Large, stiff remiges and rectrices; 2) Moderate-size, partly firm feathers that cover the body, so called contour feathers; 3) Small, fluffy down feathers; 4) Hairlike filoplumes; and 5) Tiny bristles on the face.

Some structural and mechanical properties of feathers are discussed in this chapter. For further reading, see e.g. [4], [5], [6], [7] and [8].

2.2 Remiges

The type of feathers that was tested were the remiges, also known as the flight feathers. They are the large feathers along the posterior edge of the wing and they are divided into primaries (HP) and secondaries (AP), as shown in figure 2.1. The collected feather from the birds wings was the same feather, HP1, which is the innermost primary. This is usually the first feather to be replaced during moult, and hence is the starting point of a moult sequence of the primaries. These feathers curve downward and toward the body and are about 4.5 to 5 cm long in the two studied species.

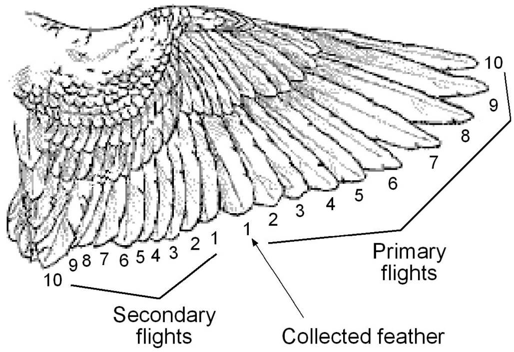

Figure 2.1: *Primaries and secondaries [3].*

2.2.1 Structure of the feather

Since the feathers are subjected to large aerodynamic forces during flight they must be stiff and strong, yet also light. Feather shafts also appears to be very strong for their weight. Damage resistance must also be good. Feathers that are lost or broken can only be replaced infrequently, but regularly at moult. According to figure 2.2 the major parts of the feather are the shaft with the vanes on each side. The shaft is composed of two segments, the calamus and the rachis. The calamus is the relatively short tubular structure that is attached to the bird and is never pigmented. It has a slightly elliptical cross-section. The rachis, which bears the vanes of the feathers, begins at the superior umbilicus where the two segments smoothly blend into each other. The color of the rachis comes from pigmentation of melanin, which is an indole pigment formed by oxidation of the amino acid tyrosine. The pigment granules containing melanin are secreted during growth into the spaces between keratin structures.

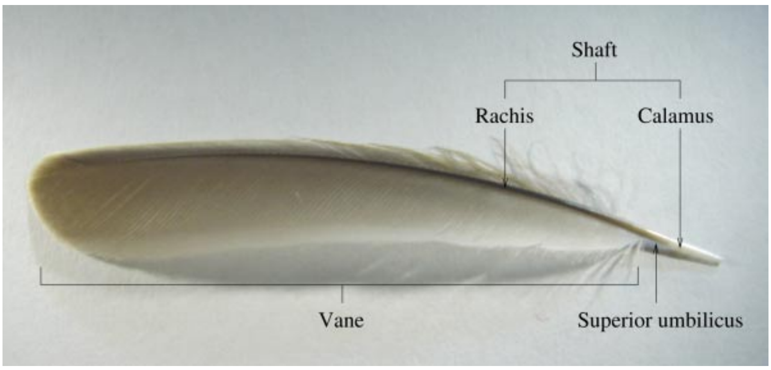

Figure 2.2: *Different parts of the feather.*

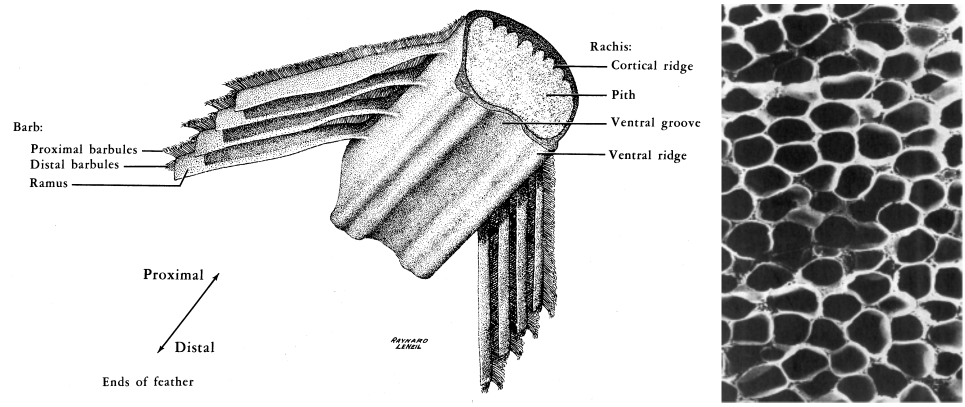

Figure 2.3: *Cross-section along the shaft of the feather [4] and a close-up of medullary foam [5].*

The cross-section of the rachis changes along the longitudinal axis. The rachis is partially filled with pith, which is a medullary foam consisting of multiangular cells with air-filled cavities, shown in figure 2.3. The size of the cells vary between 10-20 μm. On each side of the shaft is a row of closely set, fine branches that are known individually as barbs and collectively as a vane. Also the cavities within feather barbs are filled with pith. The barb consists of the ramus and proximal and distal barbules. Interlocking hooklets on the barbules give feathers their stiffness and flexibility. It is the undamaged hooklets which allows to make it whole again when fingers are run up a split vane. The vanes are asymmetrical on flight feathers, as the outer vane is narrower than the inner. Also the asymmetry between inner and outer vanes give the feather an airfoil shape. That is because there is a zone of overlap between the primary remiges, shown in figure 2.4.

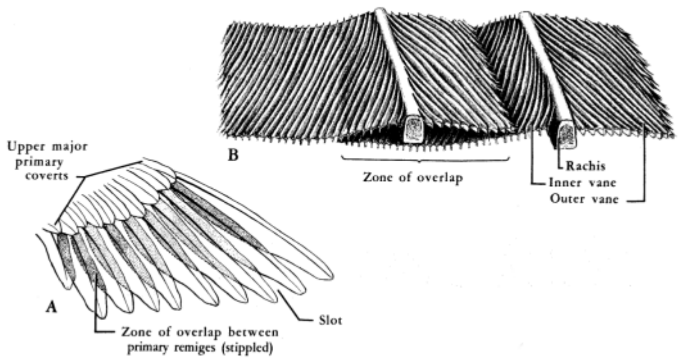

Figure 2.4: *Overlap between primary remiges [4].*

2.3 Mechanical properties overview

Attempts have been made to obtain mechanical properties of primary feathers from birds. In this section, results from earlier studies are presented.

- In simulated and observed bending of the primary feather shaft from the pigeon, the shape and size of the cortex (outer wall) of the shaft accounted for the majority of the bending stiffness. [6]
- Tensile tests on compact keratin from eight species of birds showed similar properties of the Young's modulus, E $[GPa]$, showing that the β-keratin is conservative between species. A probable mean value is E=2.50 GPa. [7]
- A study showed that the rachis of feathers exhibited two distinct layers. The orientation of keratin fibres in the inner layer was parallel to the axis of the feather. There was also a distinct outer layer, composed entirely of circumferentially oriented fibres. The outer layer constituted approximately one seventh of the thickness of the rachis wall at the base, but along the axis it became thinner. [7]
- Theoretically the cortex should be most significant to the flexural stiffness and the foam to preventing buckling. Although the foam would fulfil this function well in the rachis, the present experimental evidence is somewhat contradictory [5], except [8] that suggest that buckling is the most important mode of failure.
- Keratin and many other proteins are damaged when they are exposed to ultraviolet and visible radiation. As the energy contained in light strikes the feathers, it will begin to break molecular bonds. This is apparent as a color change and weakening or embrittlement of the fibre. [9]

Chapter 3

Experimental Study

3.1 General remarks

The objective of the experimental study was to investigate the influence of UV-radiation and mechanical wearing on the mechanical properties of feathers. The mechanical properties were determined by performing two-point bending tests measuring the bending stiffness of the feathers. Three test series were conducted. In the first series the feathers were exposed to UV-radiation (UV), in the second series the feathers were exposed to mechanical wearing (Mek), and finally, a test series was performed for a combination of feathers exposed to mechanical wearing and UV-radiation (UV-Mek). These three experiments were made on feathers from the Chiffchaff and the Willow Warbler so in total six experimental series were performed. Since the feathers were collected in May and the two bird species moult differently, the feathers from the Chiffchaff were about 9 months old and the feathers from the Willow Warbler were about 4 months old.

3.2 Bending stiffness test equipment

To measure the bending stiffness of the feathers, a test equipment for conducting two-point bending tests was constructed. The two-point bending test equipment was mounted in an MTS 810 testing machine, as shown in figure 3.1, which applied the displacement of the lower piston. The resulting bending force from the point in contact with the feather was measured with a special designed load cell.

Figure 3.1: *Bending stiffness test equipment mounted in an MTS-testing machine.*

The two-point bending test equipment consists of two parts, each consisting of a plastic cylinder and a clamping device for the feather and for the load cell respectively, as shown in figure 3.2. In the detailed drawing it is indicated that the distance from the clamp to the load was 26 *mm*. Since the feathers are about 4.5 to 5 *cm*, this means that the load was applied at a distance of about 2/3 of the feather length.

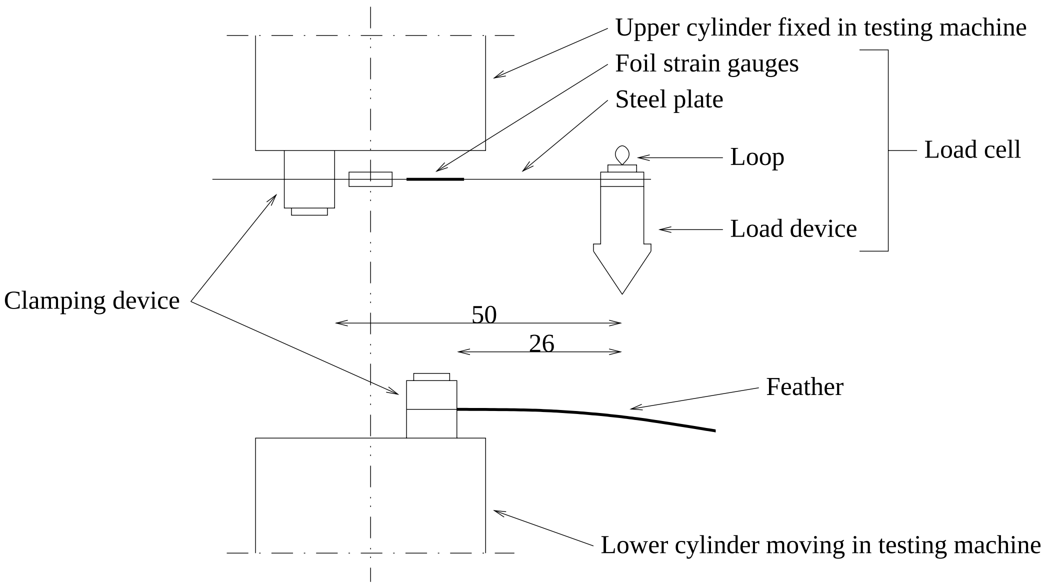

Figure 3.2: *Detailed drawing of the two-point bending test equipment.*

The force was measured from the strain of the thin steel plate clamped on the upper cylinder. To measure the strain of the thin steel plate which measured 0.2 *mm* in thickness, four foil strain gauges, two on each side, wired in a Wheatstone bridge were used. In figure 3.3 a Wheatstone bridge where opposite gauges are placed on the same side of the steel plate is shown. To be able to measure the force, the thin steel plate must bend a tiny bit. A wheatstone bridge arrangement of the foil strain gauges ensures that only the strains from pure bending of the steel plate are measured.

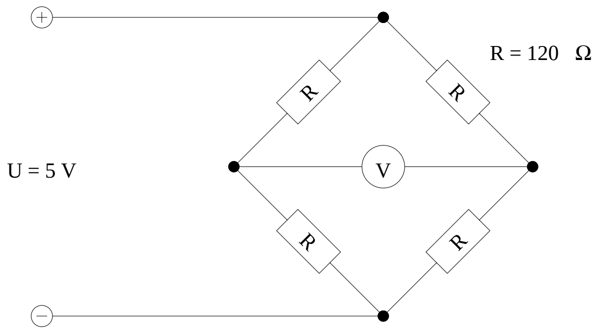

Figure 3.3: *Wiring schematic for the foil strain gauges.*

When the steel plate of the load cell bend, the resistance of the foil strain gauges change which produce a change in the voltage output. The computer then translates that to a force through a calibration constant. To calibrate the load cell it was mounted upside down and known weights were applied, as shown in figure 3.4. It was assumed that the relation between the Voltage and the force was linear in the interval of testing.

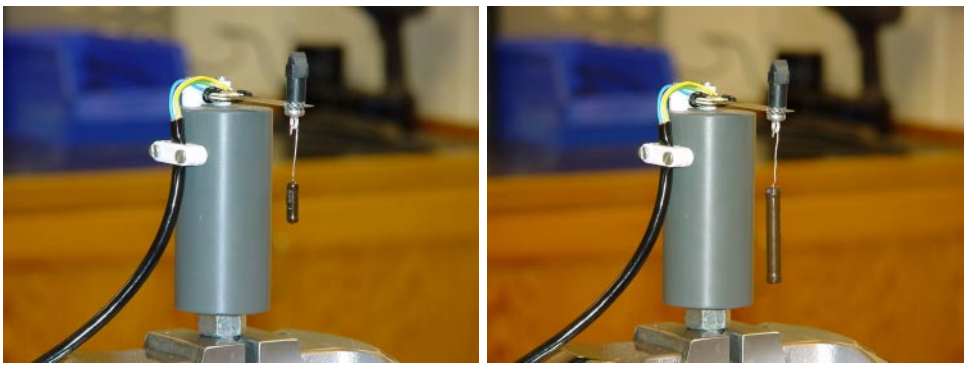

Figure 3.4: *Calibration of the load cell.*

The feathers were clamped on the lower cylinder between two ordinary cable-clamps facing each other. To prevent the feathers from twisting when the load was applied, silicone was placed on the side of the clamps that was in contact with the feather. The superfluous silicon was finished off by cutting with a razor blade. Figure 3.5 show the clamps.

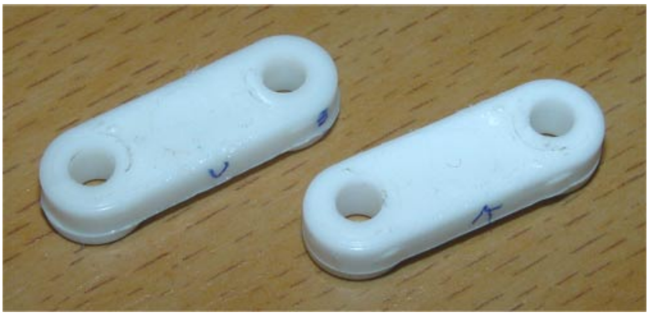

Figure 3.5: *Silicone filled clamps for mounting the feathers in the two-point bending test equipment.*

3.2.1 Bending stiffness test procedure

To investigate if the exposure of UV-radiation and mechanical wearing had any alteration effect on the bending stiffness of the feathers, the bending stiffness of each feather was measured in its original state and after each of several consequent numbers of treatments. Of practical reasons, the feathers were clamped so that they were bent downwards and curved sideways in relation to the load cell. Special care was taken to ensure that this procedure of clamping the feathers was the same for all the feathers that were tested.

The shaft of the feathers were inserted into the clamps until where the vanes begin and turned so that the load device only would touch the shaft (rachis) and not the vanes. The clamping device was tightened so that the feather didn't twist when it was loaded. The lower piston of the loading machine was then risen so that the feather barely touched the load device, as shown in figure 3.6. The loading rate was 2 *mm/min* and the data recording increment was at each 0.05 *mm*. The total test time was 3 minutes. The result of the bending stiffness test is a "live" plot and a text file with the three columns; Piston displacement [mm], Time [s] and Force [N].

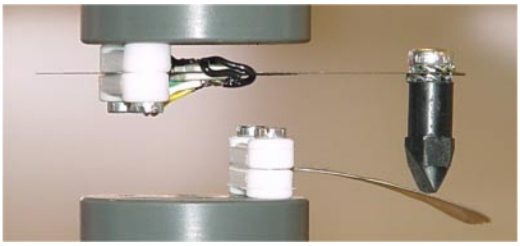

Figure 3.6: *Start position for the bending stiffness test.*

To be able to measure forces from the load cell, the thin steel plate must bend. This produce small error in the measured displacement of the feather. The error was measured by making a test with a thick steel plate instead of a feather, see figure 3.7. The displacement of the thin steel plate of the load cell was then reduced from the measurements of the feathers.

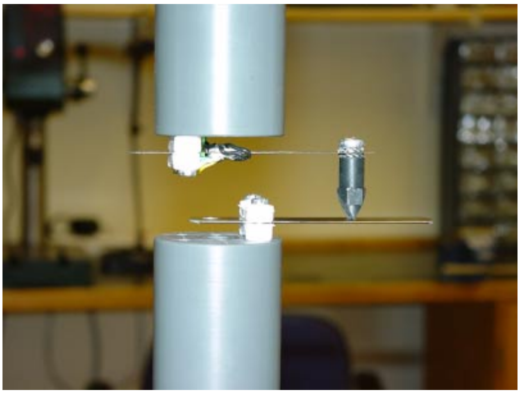

Figure 3.7: *Bending stiffness test with a steel plate.*

To analyze the recorded data the three columns were copied into an m-file in Matlab. The displacement correction was made and the force was plotted against the displacement. Figure 3.8 show the recorded and the corrected curves. A linear model was fitted to the corrected curve, y = $S_b * x + m$, and the slope, S_b of the linear fit equals the bending stiffness of the feather, see figure 3.9. This procedure was followed for all the tests.

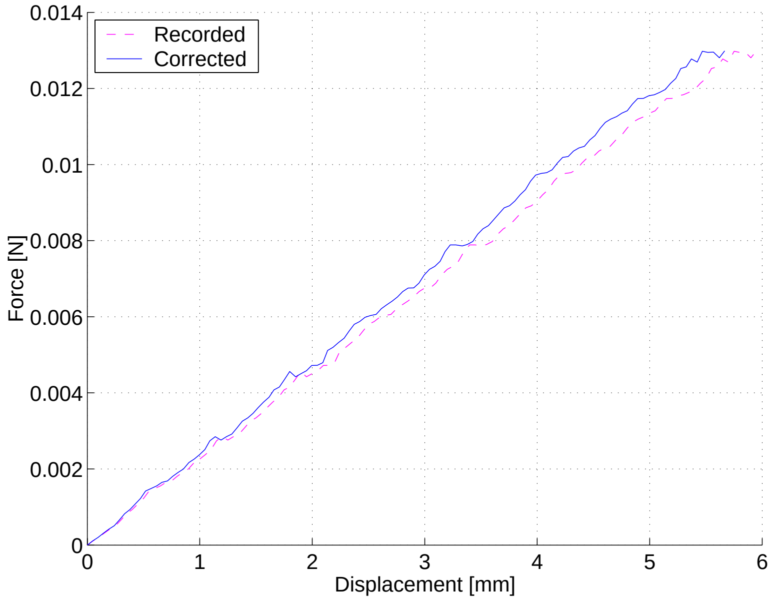

Figure 3.8: *The recorded and the corrected displacement curves.*

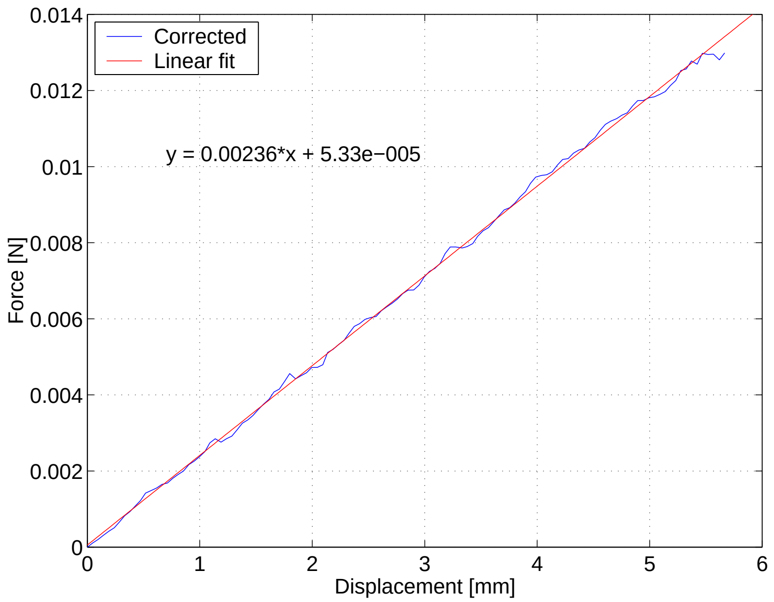

Figure 3.9: *The corrected displacement curve and a linear fit.*

3.3 UV-radiation test equipment

To investigate the influence of UV-radiation on the bending stiffness of the feathers, a UV-radiation test equipment was constructed. The objective was to expose the feathers to UV-radiation in such a manner that it was as close as possible to normal daylight exposure on the birds in their natural environment [10]. A ramp of 8 fluorescent UV-B lamps from Philips, called TL12, was used. The test setup is shown in figure 3.10.

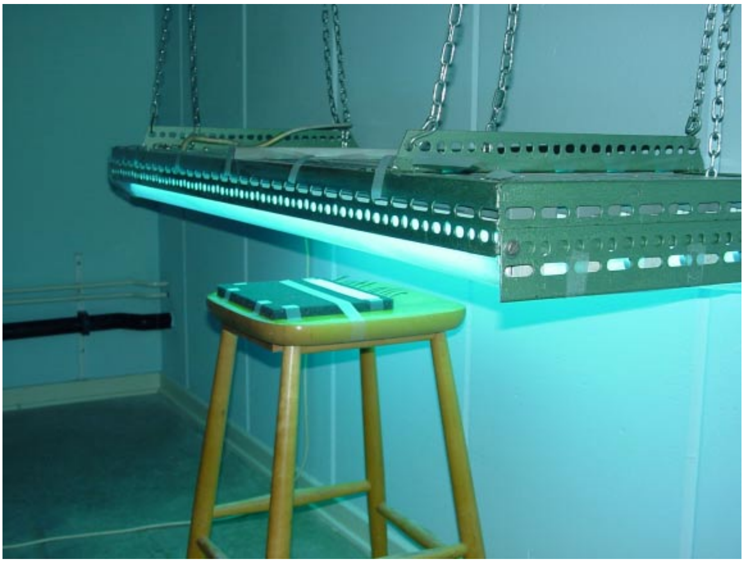

Figure 3.10: *UV-radiation test equipment.*

To get a more realistic simulation of daylight, the light was filtered through a plastic film with cellulose diacetate that reduced some of the short wave radiation. The spectral irradiance of the light was measured with a spectroradiometer at the distance from the light source that the the feathers were to be put. The resulting spectrum is shown in figure 3.11.

To be able to know the amount of UV-radiation exposure to the feathers the measured spectrum was compared with calculated daylight exposure at 23.5° Latitude (Tropic of Cancer) and 0° Longitude, which is located at West North-Africa, South Algeria, where the birds migrate during the Swedish winter. The measured spectrum was weighted against two different spectrums. A first weighting against absorption-spectrum for tryptophan, the amino acid in keratin that have strongest absorbtion of the daylight-UV, and a second against Caldwell's generalized plant action spectrum. The comparison resulted in that a one day dose corresponded to 0.972 respectively 1.46 hours of UV-radiation. This gives just a rough estimation of the UV-radiation dose and should not be taken as exact figures.

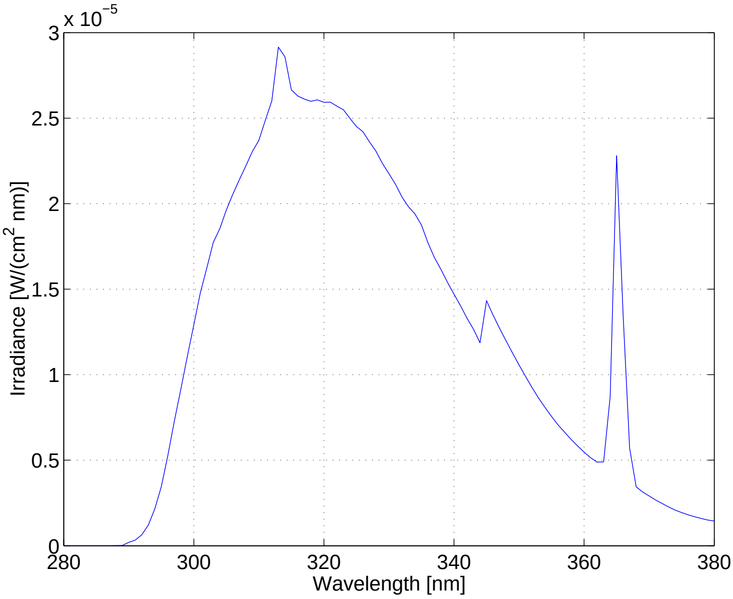

Figure 3.11: *Spectrum from the UV-radiation.*

The objective was to expose the feathers to UV-radiation as they are exposed when the birds fly and walk on the ground. Hence, the feathers were only illuminated on the convex side of the feather, which is the side that naturally gets exposed. To lift the feathers off the ground they were stuck into a porous plastic material, as shown in figure 3.12.

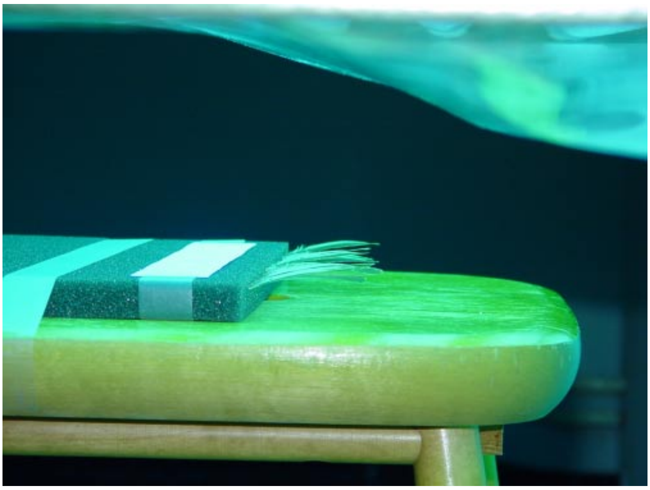

Figure 3.12: *Orientation and attachment of the feathers at UV-radiation.*

3.4 Mechanical wear test equipment

To investigate the feather shafts resistance to fatigue, a wearing test equipment was constructed, as shown in figure 3.13. It consists of an engine, a circular aluminum plate attached to the engine axis, four plastic sticks attached to the circular plate, a clamp ramp with place for four feathers and a plywood frame. The clamps were prepared with silicone as described for the clamps used in the bending stiffness test.

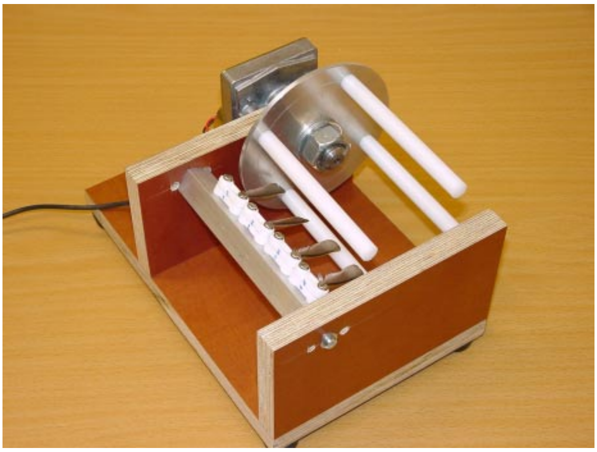

Figure 3.13: *Mechanical wear test equipment.*

To regulate the speed of the wearing a voltage regulator was connected to the engine with an adjustable output voltage from 1.5 to 12 Volts. To examine how many strokes the machine produce at a certain voltage level, the strokes were timed for one minute at 4.5, 6 and 7.5 Volts. A linear regression was made to the voltage-stroke curve in order to calculate the total number of strokes for a certain time-period.

When the birds fly they strike their wings at approximately 10 Hz. Therefore stroke speeds of the device below 10 Hz was tested. 12 V produced 6.1 strokes per second. This speed equals 21960 strokes per hour which was the speed that was chosen for all of the experiments.

During a wing strike, the feathers on the wings get bent both up and down. This behavior was simulated by turning the feathers at regular times in the clamp ramp. The adjustable parameters on the wearing device are the angular speed, the angle of the clamp ramp and the distance to the striking plastic pins. The only difference of the adjustments between the two sides of wearing was the angle of the clamp ramp. A test showed that the angle for wearing the feather bent downwards should be about 30° and for the feathers bent upwards about 45°. The shaft of the feathers were inserted into the clamps and tightened in the same way as was made in the bending stiffness test procedure. For further explanation and a more detailed description of the wear equipment see figure 3.14 and 3.15.

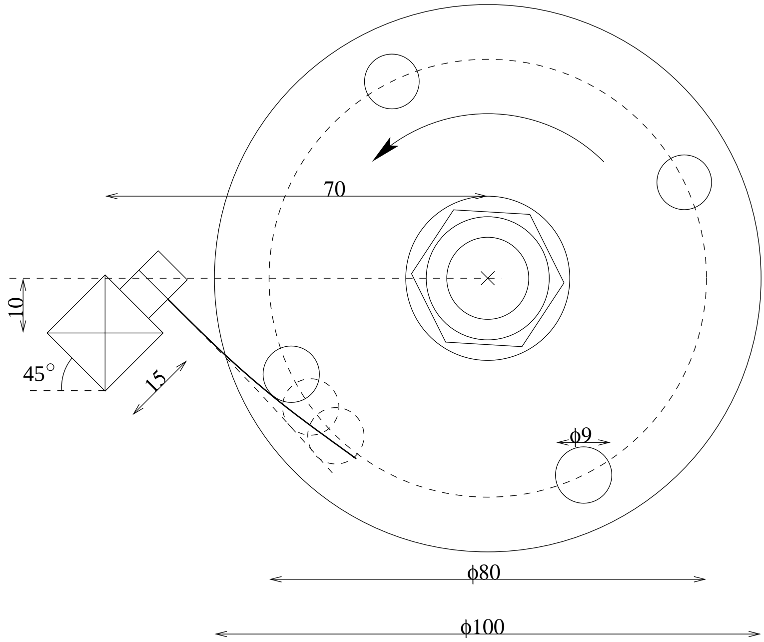

Figure 3.14: *Detailed drawing of the wear equipment describing the 45° wearing.*

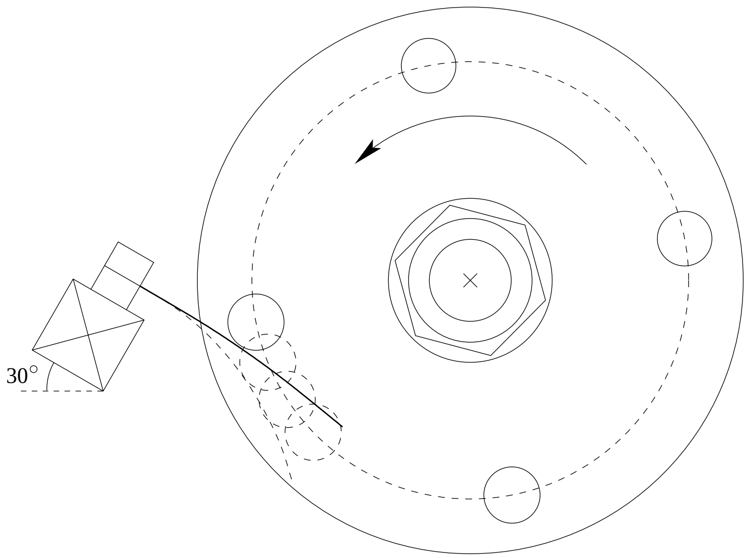

Figure 3.15: *Drawing of the wear equipment describing the 30° wearing.*

3.5 Experiments and results

3.5.1 General remarks

Three experiments were conducted. UV-radiation (UV), mechanical wearing (Mek) and a combination of the two (UV-Mek). Since the three experiments were made for each of the two bird species Chiffchaff (C) and Willow Warbler (T) this resulted in a total of six test series, CUV, CMek, CUM, TUV, TMek and TUM. All test series contained four feathers except the TMek series which only contained three because of shortage of feathers. Prior to the testing, the bending stiffness of all the available feathers of the two bird species were determined. Two diameters of each feather were also measured, a first measurement where the feathers were to be clamped and a second where the load was to be touching the feathers. The feathers for each bird species were divided into the three test series. To get the mean values of the bending stiffness of the three test series to be fairly equal, the feathers were sorted and selected by their original bending stiffness with the stiffest first, as shown in table 3.1 and 3.2. The selection of which series each feather were to belong was made according to the following procedure, A B C C B A A B C C B A. The original data, test data, measurements and sorting are showed in Appendix A. The first letter in the name of the test series origins from the first letter of the second term of the Latin name of the species. The rest of the name denotes the experimental treatment.

Table 3.1: *Test series selection for the feathers from the Chiffchaff (C) and the Willow Warbler (T).*

Test no.	Bending stiffness	Series no.
4	0.00255	CUV1
7	0.00239	CMek1
8	0.00237	CUM1
5	0.00189	CUM2
11	0.00171	CMek2
13	0.00150	CUV2
12	0.00146	CUV3
6	0.00192	CMek3
10	0.00132	CUM3
9	0.00131	CUM4
3	0.00124	CMek4
2	0.00095	CUV4

Test no.	Bending stiffness	Series no.
11	0.00544	TUV1
2	0.00449	TMek1
10	0.00409	TUM1
6	0.00399	TUM2
1	—	TMek2
9	0.00334	TUV2
5	0.00331	TUV3
3	0.00306	TMek3
12	0.00295	TUM3
7	0.00279	TUM4
8	0.00263	TMek4
13	0.00240	TUV4

Table 3.2: *The bending stiffness mean values of the six test series.*

Latin name	Species	UV	Mek	UV-Mek
*Phylloscopus **c**ollybita*	C	0.001615	0.001815	0.001723
*Phylloscopus **t**rochilus*	T	0.003623	0.003470	0.003455

In table 3.3 the number of feathers in each test series are displayed.

Table 3.3: *Number of feathers in each test series.*

Experiment	Chiffchaff	Willow Warbler
UV	**4×CUV**	**4×TUV**
Mek	**4×CMek**	**3×TMek**
UV-Mek	**4×CUM**	**4×TUM**

In this chapter, the results from the three bending stiffness experiments are shown as mean values of all the feathers in the same series. The results of the bending stiffness tests for all the feathers in respective series are shown in Appendix B.

3.5.2 UV-radiation

To determine the exposure time between each bending stiffness test, the first two bending stiffness tests were performed after 24h and 72h of exposure. The conclusion was to irradiate for 48h followed by a bending stiffness test which completed one session of (UV). In table 3.4 the sessions and the estimated dosage for the UV-radiation experiment are displayed. The first dosage was calculated with the absorbtion spectrum for tryptophan and the alternative dosage was calculated from Caldwell's generalized plant action spectrum.

Table 3.4: *Sessions and dosage of the UV-radiation experiment.*

Session	UV [h]	Dose [year]	Alt. Dose [year]
1	24	0.07	0.05
2	72	0.20	0.14
3	120	0.34	0.23
4	168	0.47	0.32
5	216	0.61	0.41
6	264	0.74	0.50
7	312	0.88	0.59
8	360	1.01	0.68
9	408	1.15	0.77
10	456	1.29	0.86
11	504	1.42	0.95
12	552	1.56	1.04
13	600	1.69	1.13
14	648	1.83	1.22

The visual effects of this experiment was a color change of the shaft which occurred after long exposure to UV-radiation. The bleaching of the melanin on the feather shaft being the most significant, as shown in figure 3.16. When the feathers were observed in a microscope, obvious cracks in the cortex of the calamus were discovered. This was not detected in untreated feathers and probably occurred because of the clamping in the two point bending test.

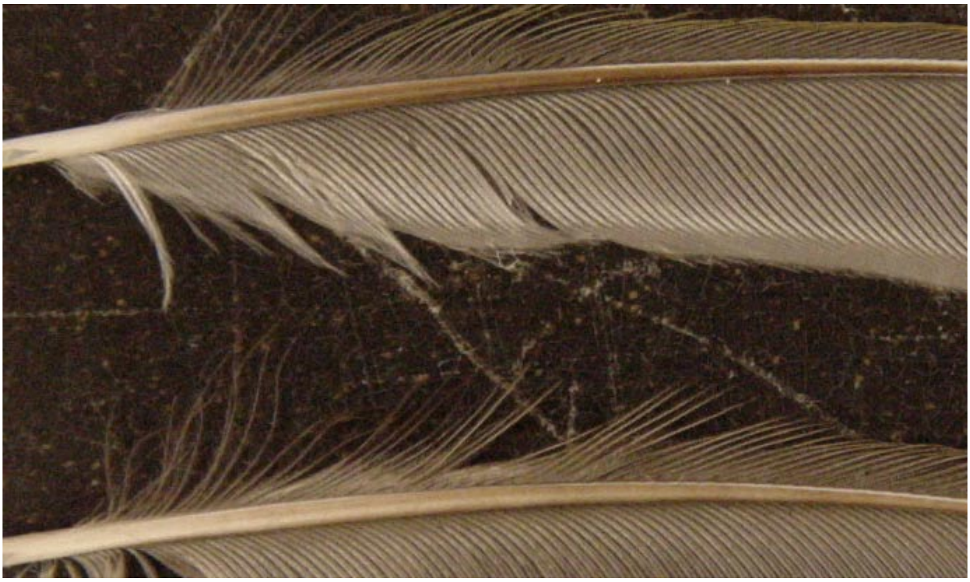

Figure 3.16: *Visual bleach of the lower feather exposed to UV-radiation.*

Results from the UV-radiation experiment

In figure 3.17 and 3.18 the results from the UV-experiment are shown. It is evident that the trend and behavior of the bending stiffness change are the same for the two species. For short UV-radiation exposures the bending stiffness increases to reach a maximum bending stiffness for exposures of about 200 hours. For further increasing UV-radiation exposures, the bending stiffness decreases rapidly below the original bending stiffness values.

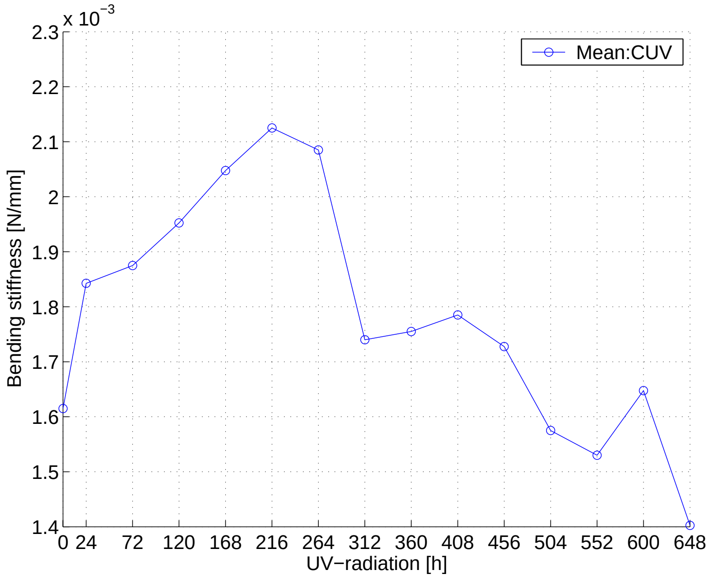

Figure 3.17: *Mean values of bending stiffness tests after UV-radiation on the feathers of the Chiffchaff.*

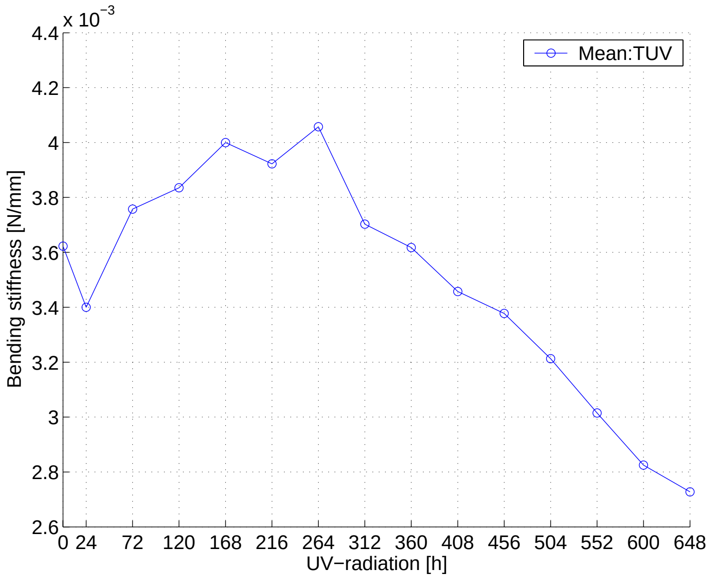

Figure 3.18: *Mean values of bending stiffness tests after UV-radiation on the feathers of the Willow Warbler.*

3.5.3 Mechanical wearing

The idea of the mechanical wearing was to bend the feathers in a natural way to introduce fatigue in the shaft. To know how many strokes of wearing that were to be applied to the feather between the bending stiffness tests were performed, bending stiffness tests were performed after one, three, five and seven hours of wearing, turning the feather each hour. The conclusion was to wear for four hours, turning the feathers each hour, and then do a bending stiffness test, which completed one session of (Mek). In table 3.5 the sessions and number of strokes for the mechanical wear experiment are displayed.

Table 3.5: *Sessions and number of strokes for the Mechanical wear experiment.*

Session	Mek [h]	Strokes [n]
1	5	110000
2	9	198000
3	13	286000
4	17	374000
5	21	462000
6	25	550000
7	29	638000
8	33	726000
9	37	814000
10	41	902000

No visible changes of the feather shaft could be found on the feathers undergoing the wearing procedure compared to untreated feathers, except cracks in the calamus because of the clamping. When the birds migrate to Africa they strike their wings approximately 15 million times. In this test, the feathers were subjected to a total of 900 000 strokes which is quite few in comparison. However the loading conditions applied in this test may be worse than the loading during normal flight.

Results from the Mechanical wearing experiment

The results of the mechanical wear-experiment is shown in figure 3.19 and 3.20. The trend is alike for the two species showing that the stiffness decreases constantly for an increase in number of strokes.

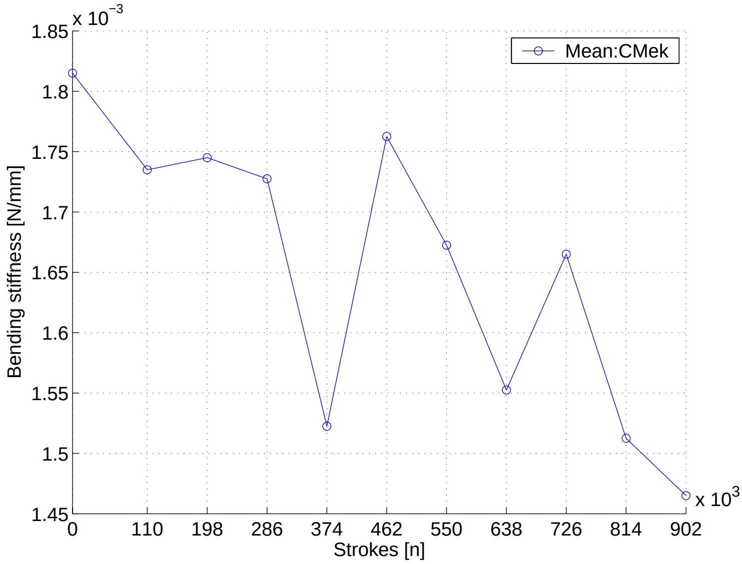

Figure 3.19: *Mean values of bending stiffness tests after mechanical wearing on the feathers of the Chiffchaff.*

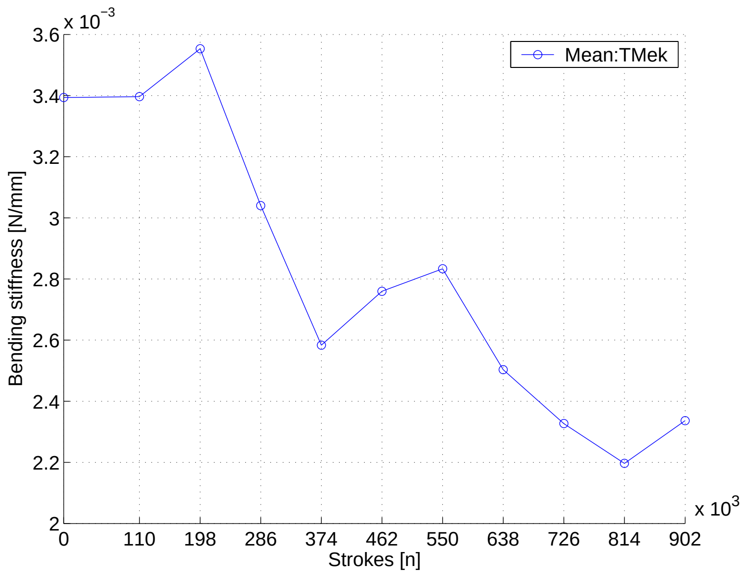

Figure 3.20: *Mean values of bending stiffness tests after mechanical wearing on the feathers of the Willow Warbler.*

3.5.4 UV-radiation and mechanical wearing

In this experiment the objective was to investigate if the combination of UV-radiation and mechanical wear gave a different alteration effect on the bending stiffness than the single experiments alone. The intervals to expose the feathers to treatments were in this test selected in the same manner as for the single UV- and mechanical experiments. Table 3.6 show the sessions of this experiment.

Table 3.6: *Sessions of the combined experiment.*

Session	Experiment	UV [h]	Strokes [n]
1	UV	24	
2	Mek		110000
3	UV	72	
4	Mek		198000
5	UV	120	
6	Mek		286000
7	UV	168	
8	Mek		374000
9	UV	216	
10	Mek		462000
11	UV	264	
12	Mek		550000
13	UV	312	
14	Mek		638000
15	UV	360	
16	Mek		726000

Results from the UV-radiation and Mechanical wearing experiment

The results of the combined experiments are shown in figure 3.21 and 3.22. Here the bending stiffness test has been made after each experiment, with UV-radiation first, followed by mechanical wearing. In figure 3.22 an interesting trend can be observed in the middle of the curve. For four sessions after 198000 strokes there is an indication that the UV-radiation makes the feathers stiffer and the mechanical wearing makes them softer. The increase in bending stiffness during the UV-radiation phase is very small though.

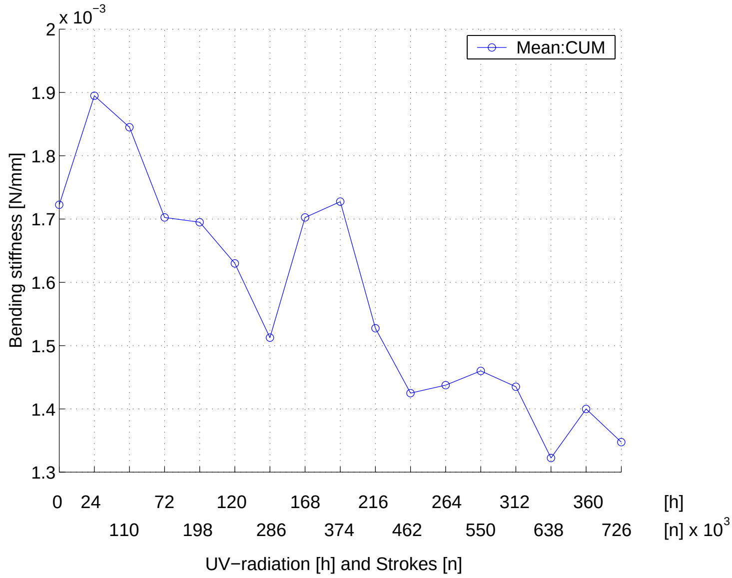

Figure 3.21: *Mean values of bending stiffness tests after UV-radiation and Mechanical wearing on the feathers of the Chiffchaff.*

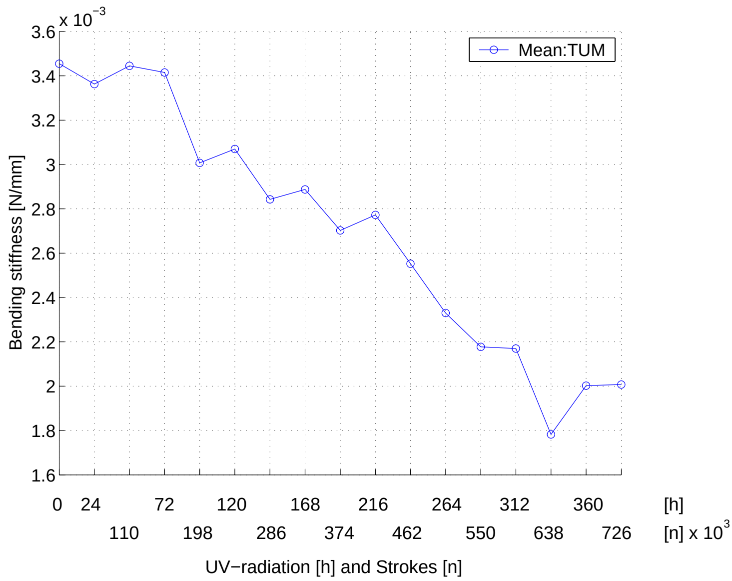

Figure 3.22: *Mean values of bending stiffness tests after UV-radiation and Mechanical wearing on the feathers of the Willow Warbler.*

3.6 Discussion

To compare the results between the two bird species, all the bending stiffness values in each series were divided by the bending stiffness values determined for untreated feathers. This procedure allow the study of the bending stiffness change instead of the absolute bending stiffness values. Since all the values are compared with the original bending stiffness value, it is of importance that the original value is a "true" value, otherwise the comparison made to the rest of the values is made with a wrong value. However, since the mean values of the results from the bending stiffness tests were used, the error is somewhat minimized.

3.6.1 Comparisons between bird species

In the following five figures, comparisons of the change in bending stiffness obtained for the two bird species are shown. The comparison of the change in bending stiffness due to UV-exposure for the two bird species is shown in figure 3.23.

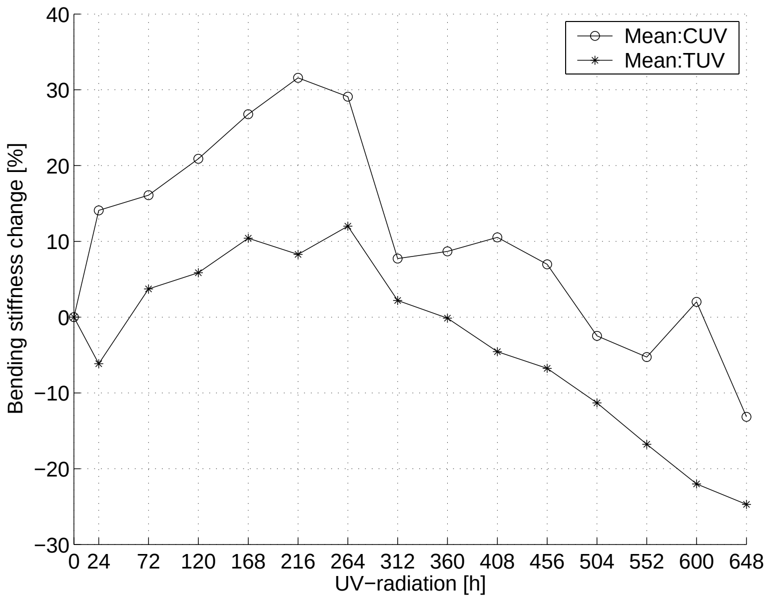

Figure 3.23: *Comparison of the two bird species for the UV-experiment.*

The difference between the two bird species in the UV-experiment is very low. The curves are just displaced vertically. This is because of the comparison with the first value. The problem of spread in the first values has occurred because of initial uncertainties in the stiffness test procedure. The effect of UV-radiation on the bending stiffness is that the stiffness first increases then to be decreasing below the initial bending stiffness.

The comparison of the two bird species for the mechanical wear experiments is shown in figure 3.24. The comparison shows the existence of a difference between the two species. The bending stiffness decreases more rapidly for the Willow Warbler than for the Chiffchaff. This result indicates that the biannual moulting Willow Warbler has feathers with slightly poorer quality than the Chiffchaff.

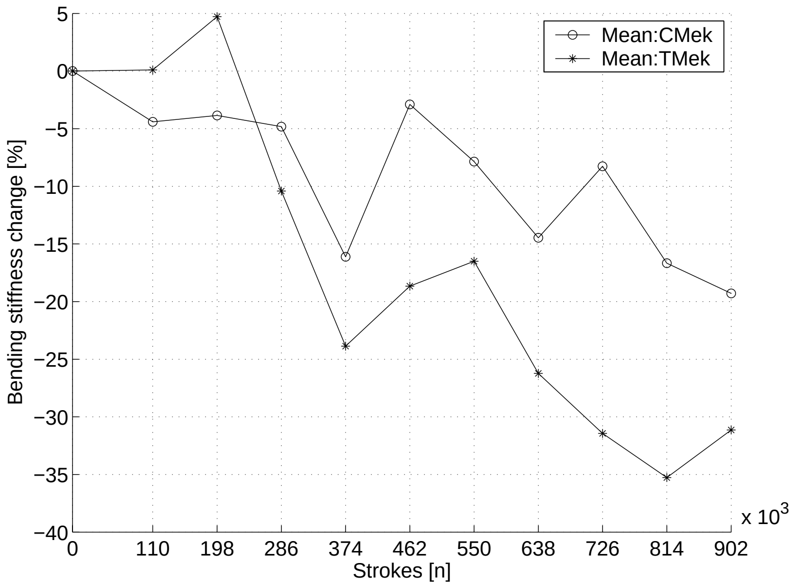

Figure 3.24: *Comparison of the two bird species for the Mechanical wear-experiment.*

The comparison of the two bird species for the combined experiments is shown in figure 3.25. Also for the combined experiment a difference between the two species may be distinguished. The bending stiffness decreases more rapidly for the Willow Warbler than for the Chiffchaff as was the case in the single Mek experiment.

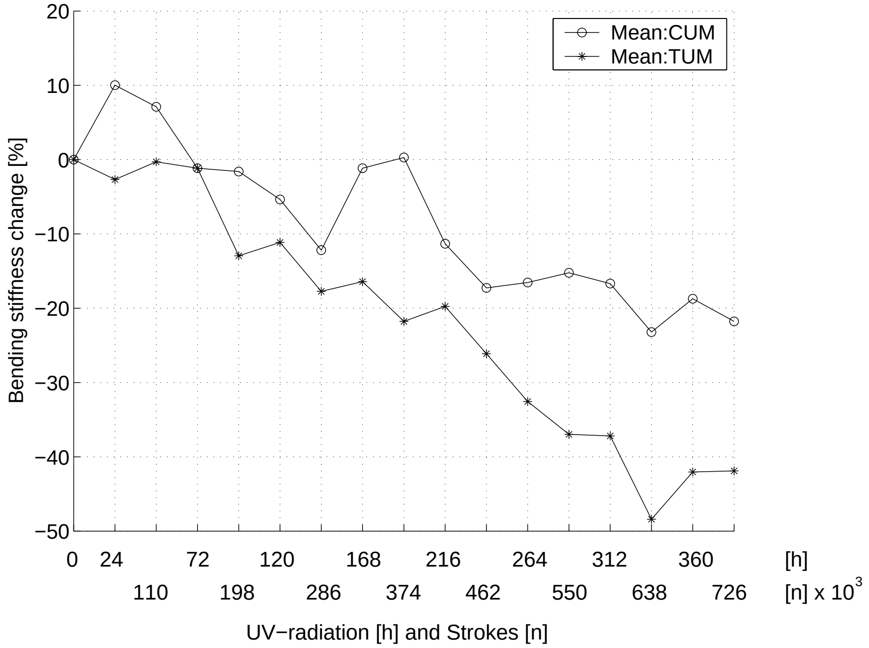

Figure 3.25: *Comparison of the two bird species for the combined experiment.*

To compare the UV- and the mechanical experiment separately in the combined experiment, the relative bending stiffness values were isolated for the two different types of experiment, as shown in figure 3.26 and 3.27.

Studying the UV part only, no differences in bending stiffness change of the two bird species were found for this treatment of the feathers, see figure 3.26

Studying the Mek part only, the bending stiffness was found to decrease more rapidly for the Willow Warbler than for the Chiffchaff as was the case in the single Mek experiment, see figure 3.27.

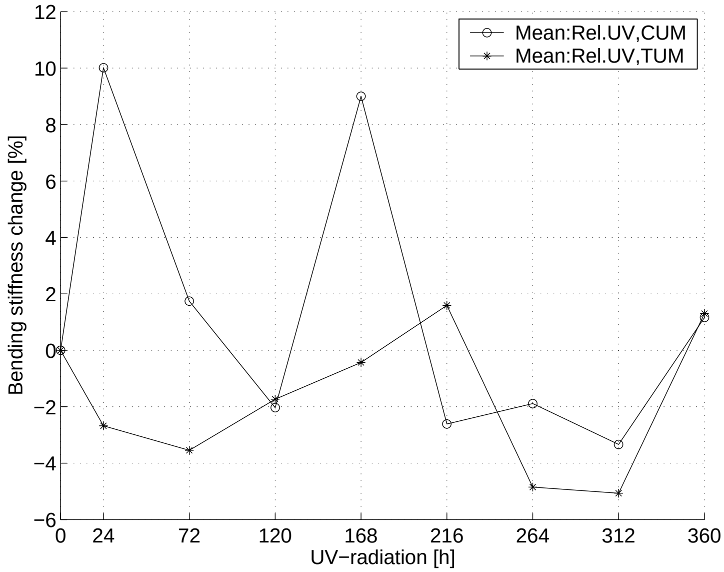

Figure 3.26: *Comparison of the relative bending stiffness change for the two bird species studying the UV part in the combined experiment only.*

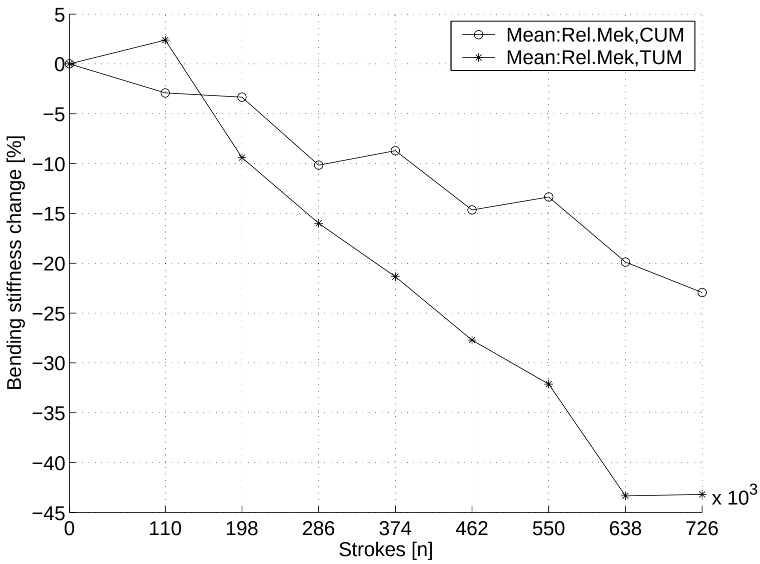

Figure 3.27: *Comparison of the relative bending stiffness change for the two bird species studying the mechanical part in the combined experiment only.*

3.6.2 Comparisons between experiments

The following four figures show comparisons of the single and combined experiments. The comparison between the UV experiment and the UV part of the combined experiment on the Chiffchaff is shown in figure 3.28. The increasing effect of UV-radiation on the bending stiffness as in the single experiment is completely missing in the UV part of the combined experiment. It is evident that the Mechanical wear part of the combined experiment prevents the UV part to make the feathers stiffer as was found in the single UV experiment.

The comparison of the mechanical wear experiment and the mechanical wear part of the combined experiment on the Chiffchaff is shown in figure 3.29. A slight difference between the experiments may be distinguished. The mechanical wear part of the combined experiment was found to have a slightly larger bending stiffness change than the single mechanical wear experiment.

The comparison of the UV experiment and the UV part of the combined experiment on the Willow Warbler is shown in figure figure 3.30. The same difference between the experiments appears here as for the same comparison between experiments on the Chiffchaff. The increasing bending stiffness for increasing UV-radiation as was found in the single experiment is completely missing when studying the UV part of the combined experiment.

The comparison of the mechanical wear experiment and the mechanical wear part of the combined experiment on the Willow Warbler is shown in figure 3.31. The same difference between the experiments appears here as for the same comparison between experiments on the Chiffchaff. The mechanical wear part of the combined experiment was found to have a slightly larger bending stiffness change than the single mechanical wear experiment.

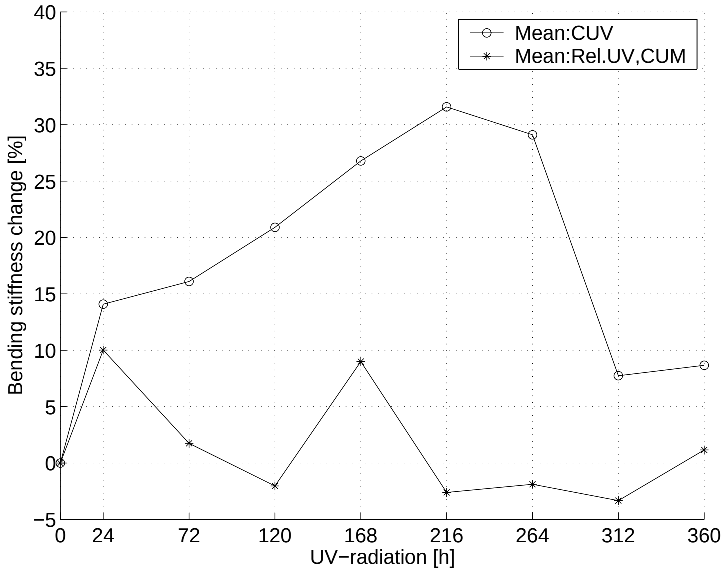

Figure 3.28: *Comparison of the UV experiment and the UV part of the combined experiment on the Chiffchaff.*

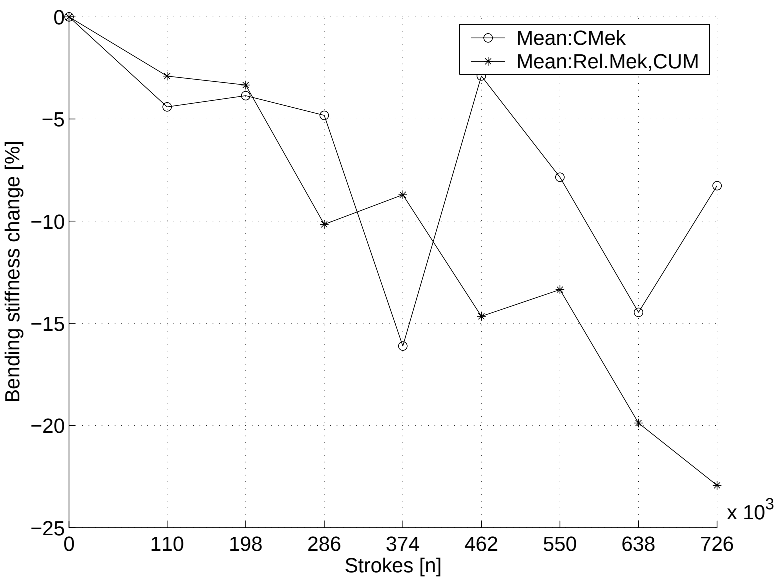

Figure 3.29: *Comparison of the mechanical experiment and the mechanical part of the combined experiment on the Chiffchaff.*

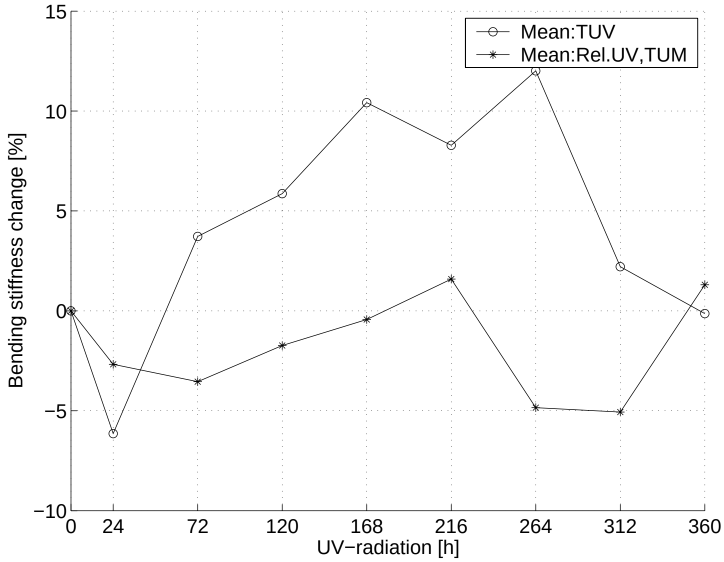

Figure 3.30: *Comparison of the UV experiment and the UV part of the combined experiment on the Willow Warbler.*

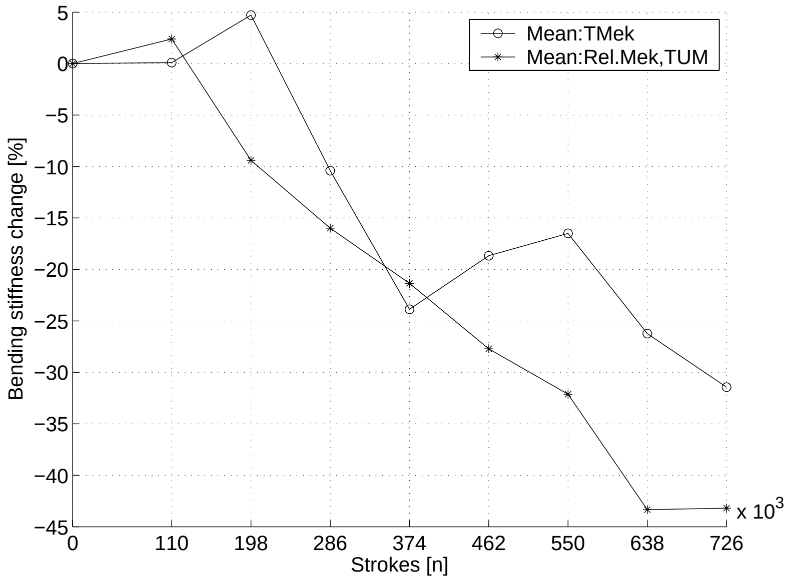

Figure 3.31: *Comparison of the mechanical experiment and the mechanical part of the combined experiment on the Willow Warbler.*

3.6.3 Concluding remarks

The cracks that developed in the shaft due to the clamping were regarded not to interface with the measurements since both decreasing as well as increasing stiffnesses were obtained.

Comparisons between bird species

In the single experiments no differences among the two species were found in the bending stiffness change for the UV treatment of the feathers. In the mechanical wear experiment slight differences were distinguished, where the bending stiffness decreased more rapidly for the Willow Warbler than for the Chiffchaff.

In the combined experiment, the same trend as presented above was found analyzing the UV- and the mechanical wear parts alone. Still, the combined experiment showed that the total bending stiffness decreased more rapidly for the Willow Warbler than for the Chiffchaff.

Comparisons between experiments

When comparisons between the different types of experiments were made, the same differences were found for the two bird species. The increasing effect of UV-radiation on the bending stiffness as was found in the single experiment was completely missing in the UV part of the combined experiment.

The mechanical wear part of the combined experiment was found to have a slightly larger bending stiffness change than the single mechanical wear experiment.

Chapter 4

FE-Modelling

4.1 General remarks

The objective of the FE-modelling was to evaluate the Young's modulus, E and analyzing torsional effects by comparing the results of the bending stiffness test procedure with a FE-simulation. Since the structure of the feather is very complex a simplified model was constructed. The conclusions of earlier studies is that the bending stiffness is mainly governed by the cortex of the feather shaft, whereas the pith within the shaft is shown to have very little importance [6]. The vanes were assumed not to contribute to the bending stiffness in the region of the feather that was studied. Based on these facts the feather shaft was modelled without pith and vanes.

Firstly, a geometry model was created from pictures and micrographs of a feather shaft from the Chiffchaff. For the geometry modelling a program called Solid Works 2001 Plus was used. Secondly, a FE-model was created. The geometry model was imported into the pre-processor MSC Patran 2001 r3, where a FE-mesh was created, loads and boundary conditions were prescribed, a material was applied and finally an input file for ABAQUS/Standard version 6.3 was created. The input file for ABAQUS is shown in Appendix C. Thirdly, an analysis was made in ABAQUS. The FE-program ABAQUS execute the commands in the input file and finds a solution to the problem. The results were visualized in the post processor ABAQUS Viewer.

Since this analysis was made on a structure where large deformations occur, a nonlinear analysis was performed. A geometric nonlinear analysis is based on equilibrium on deformed geometry. This type of analysis is requested by including the ABAQUS option *NLGEOM in the input file.

4.2 Geometry model

A three-dimensional geometry model of a feather shaft was created from photographs and micrographs of the shaft of a feather from the Chiffchaff. Firstly, the curvature of the main axis of the shaft was modelled from photographs of the feather from the top and the side with a scale. The pictures were imported into Solid Works and two-dimensional centerlines were created for the shaft in the xz- and yz-plane, as shown in figure 4.1. Secondly, cross-sections at 15 locations along the main axis was modelled from micrographs, as shown in figure 4.2. The three-dimensional geometry model was then created by interpolating the geometry between each section, as shown in figure 4.3.

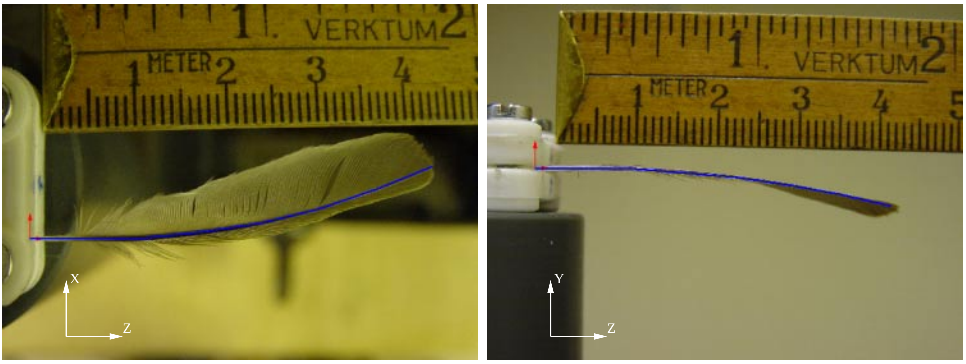

Figure 4.1: *Feather photographed in the xz- and yz-plane from which the two-dimensional centerlines were created.*

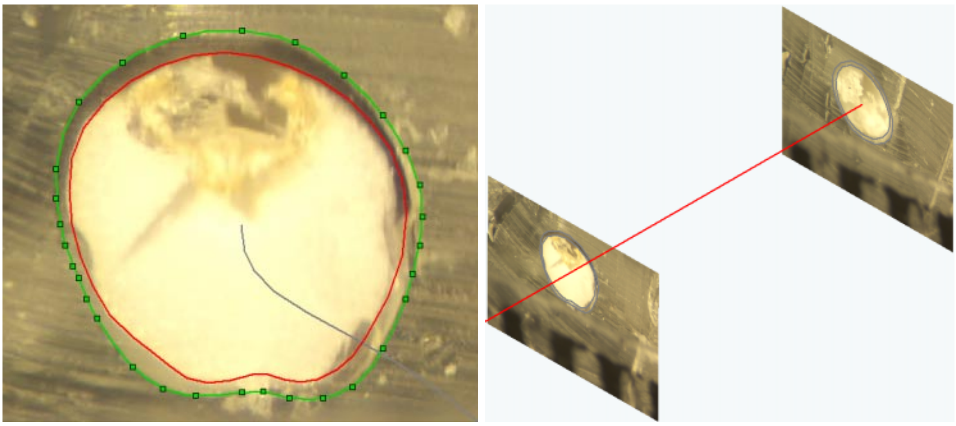

Figure 4.2: *Geometry of the cross-sections created from micrographs.*

Figure 4.3: *The three-dimensional geometry model created from micrographs of cross-sections. The cross-sections are indicated to the left and the final geometry to the right.*

4.2.1 Micrographs of cross-sections

To make the cross-sections the feather was embedded in epoxy resin in a cast box. To fix the feather in the box a hole was drilled in the center of each short side of the box, a tiny thread was glued to each end of the feather, the threads were stuck into each hole and the sides were taped. The feather was stretched as straight as possible to get perpendicular cuts of the shaft. At last the epoxy resin was mixed and the box was filled. The resin hardened for a couple of weeks before sawing the cross-sections. The embedded feather is shown in figure 4.4.

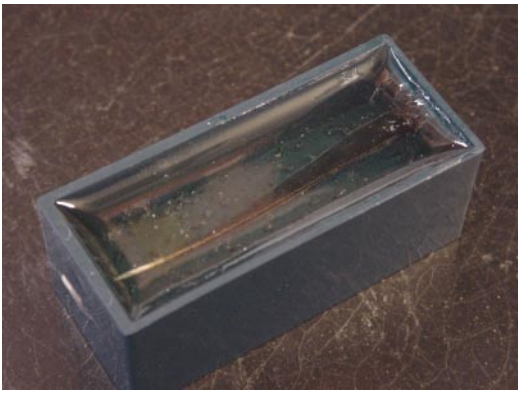

Figure 4.4: *Feather embedded in epoxy resin.*

Cross-sections were cut with a band saw using a 1 *mm* blade for plastic objects. The cross-sections were cut 2 *mm* thick giving 17 sections and 34 sides. Since the saw blade produced rough surfaces the cross-sections were finished off with a cut from a razor blade. The micrographs were made by placing each cross-section in a microscope fitted with a digital camera, taking them together with a scale. The micrographs of the cross-sections are shown in figure 4.7 and 4.8, where the positions displayed are related to the whole feather length. Because of the limitations of the microscope and the digital camera, the micrographs couldn't be sharper or more enlarged than displayed. Another problem was that the epoxy resin shrunk and deformed the cross-sections of the feather.

4.3 Finite Element model

An introduction to the Finite Element Method is described in [11]. The method can be used to solve force-displacement problems as in this case. The aim of the simulation was to simulate the two-point bending test and compare the resulting force-displacement plot with experimental data.

A finite element model of the shaft was created from the imported geometry model by using the pre-processor MSC Patran. Since the force was applied at 26 *mm* from the fixed end of the shaft, only 30 *mm* of the geometry model was meshed.

Element type and mesh

The geometry model of the shaft was meshed with the element type C3D8 which is an 8-node iso-parametric solid element. Since the structure was fairly complex and it was difficult to get a good mesh of the shaft, different types of elements were tested. To ensure a good solution, a fine mesh with 12000 elements was employed. The meshed feather shaft is shown in figure 4.5 and a close up in figure 4.6.

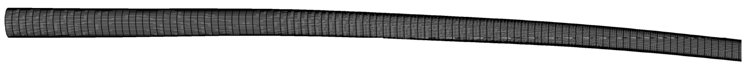

Figure 4.5: *Meshed feather shaft.*

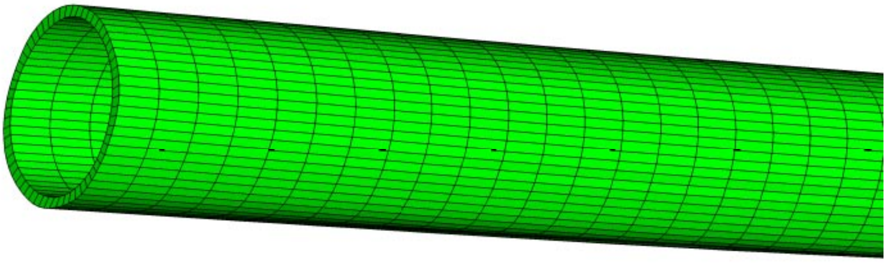

Figure 4.6: *Close up of mesh.*

Boundary conditions and material

Since no symmetry planes could be defined the entire feather had to be modelled except for the bit stuck into the clamps. Hence, the model begins where the clamping ends. All nodal displacements for the model in the plane at the clamp were prescribed to zero.

The material of the cortex is made of keratin. Keratin is reported as being an oriented material and is probably orthotropic. But since no such material data is available in the literature the material was assumed isotropic with a Young's modulus, E= 2.5 GPa and Poisson's ratio, ν= 0.3. The Young's modulus was taken as the mean value from an earlier study of different bird species [7].

Load case

The load was simulated with a ramp from 0 to -5 mN, oriented in the y-direction. To simulate the loading in the two-point bending test the load was divided over five nodes at a distance of 26 mm from the clamp.

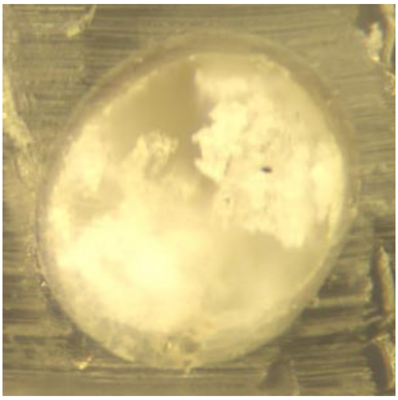

Position= 6 *mm*
Diameter= 0.62 *mm*

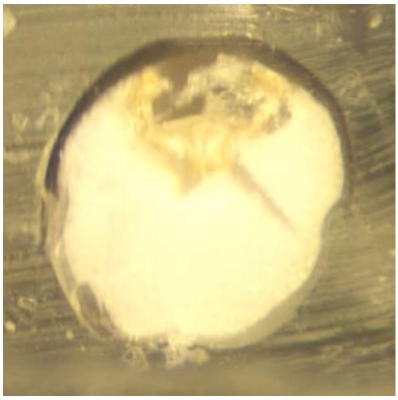

Position= 9 *mm*
Diameter= 0.61 *mm*

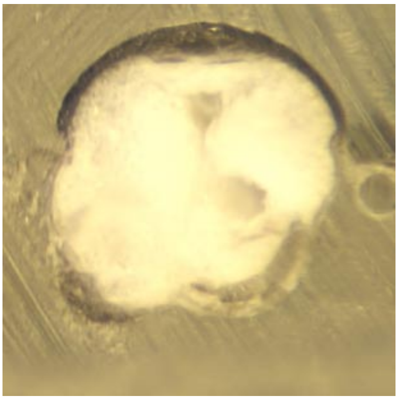

Position= 12 *mm*
Diameter= 0.57 *mm*

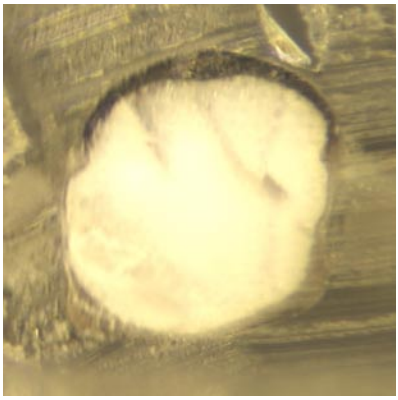

Position= 15 *mm*
Diameter= 0.52 *mm*

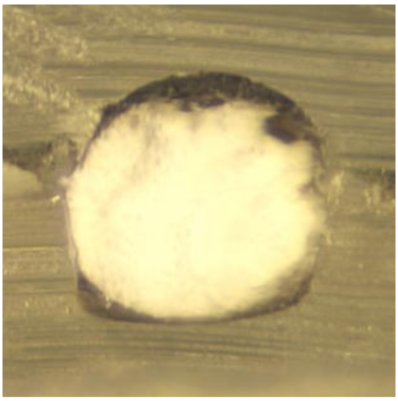

Position= 21 *mm*
Diameter= 0.50 *mm*

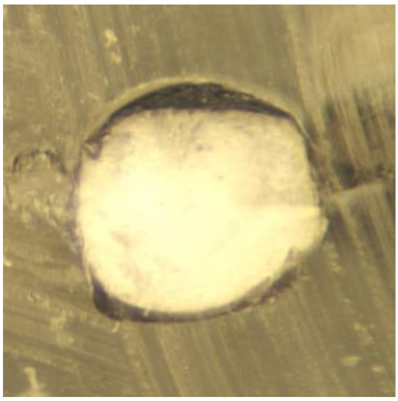

Position= 24 *mm*
Diameter= 0.47 *mm*

Figure 4.7: *Micrographs of cross-sections.*

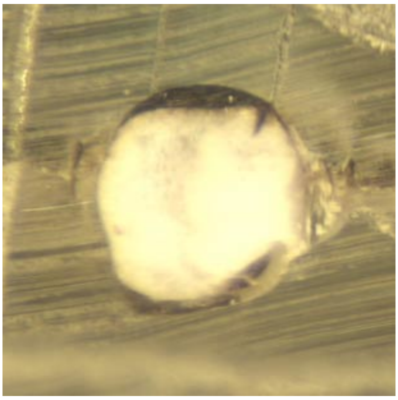

Position= 29 mm
Diameter= 0.41 mm

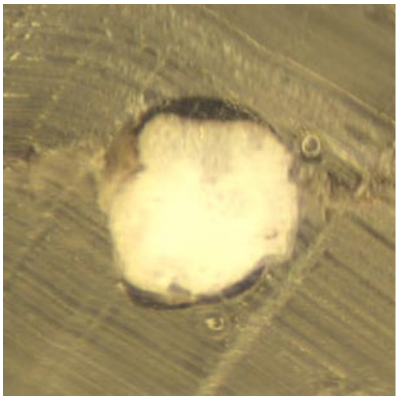

Position= 32 mm
Diameter= 0.37 mm

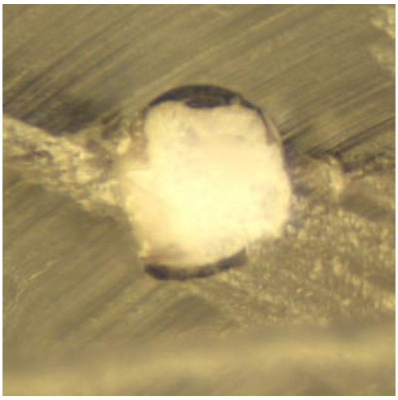

Position= 35 mm
Diameter= 0.32 mm

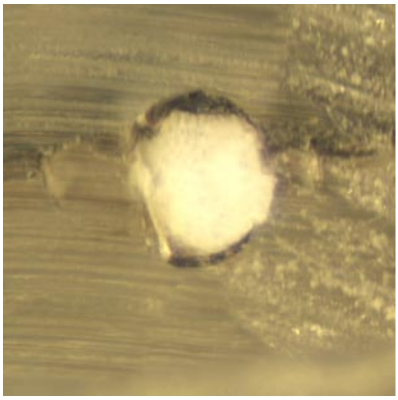

Position= 38 mm
Diameter= 0.29 mm

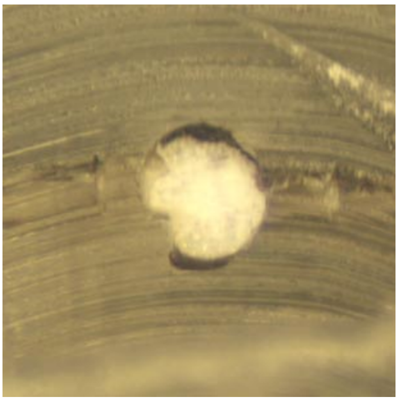

Position= 41 mm
Diameter= 0.25 mm

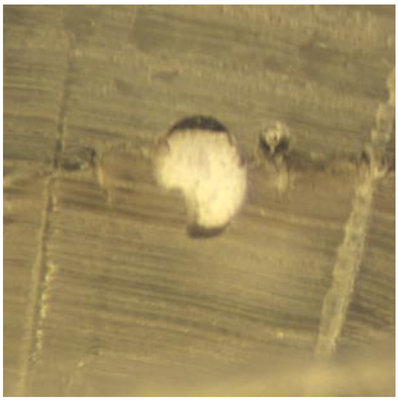

Position= 44 mm
Diameter= 0.19 mm

Figure 4.8: *Micrographs of cross-sections.*

4.4 Results from the FE-simulation

The FE-simulation produces a solution to the problem which can be visualized in a post processor. In figure 4.9 the undeformed and deformed feather shafts are shown.

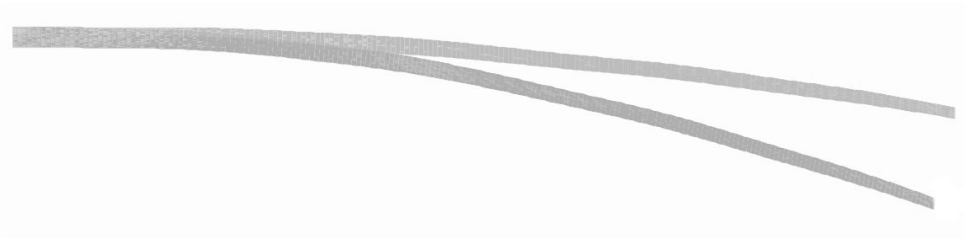

Figure 4.9: *Results from the FE-simulation showing the undeformed and deformed feather shafts.*

From the result of the simulations, a force versus displacement graph was plotted. The result from the simulation is shown in figure 4.10. As evident, the curve is quite linear and shows a displacement just over 5 *mm* at a load of 5 *mN*. Maximum stress, σ_{max}= 15.1 *MPa*.

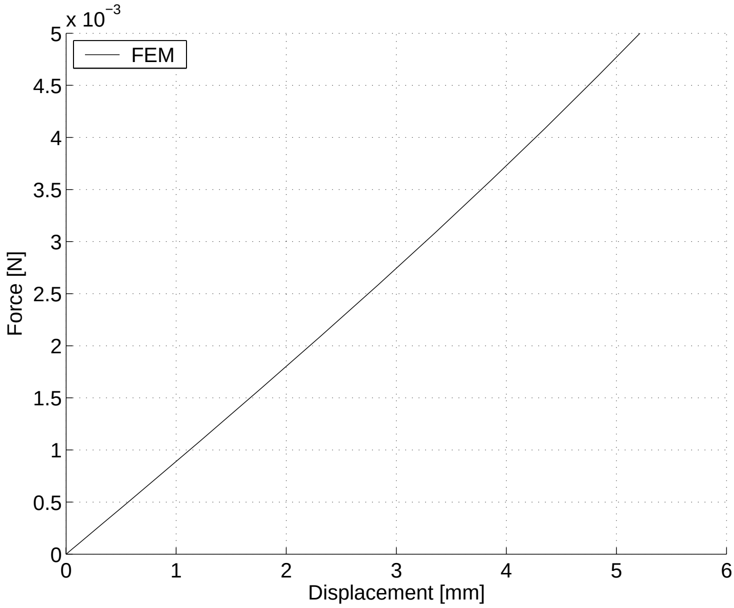

Figure 4.10: *Results from the FE-simulation.*

4.5 Comparison with the bending stiffness test

The comparison is made with the bending stiffness test result from the exact same feather that was modelled. To compare the FE-simulation with the bending stiffness test the two force-displacement curves were plotted together as shown in figure 4.11. A linear model was fitted to the curves and the slopes, S_b, were compared. As evident, the curves are separated but the slopes of the linear fits are very similar. In this case the difference between the slopes is less than 1 %.

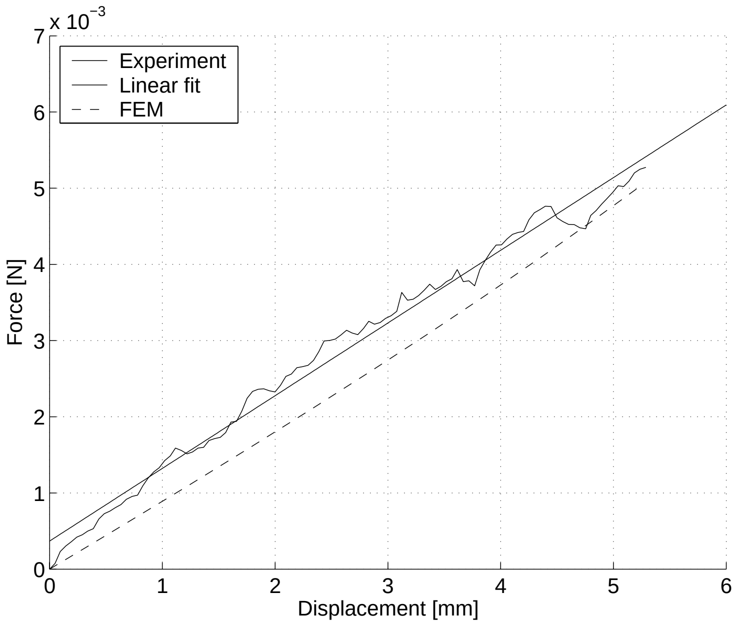

Figure 4.11: *Comparison of FE-simulation and experimental results.*

4.6 Discussion

The FE-modelling was very delayed in the project. Hence the analysis is not entirely satisfying and as thorough as it was meant to be. Although the results from the comparison shows very good agreement. A Young's modulus, E= 2.5 *GPa*, taken from an earlier study is most likely a good value. Moreover, the analysis also shows that the pith is insignificant to the bending stiffness. In this analysis, the torsion produced by applying a vertical load was minimal.

Chapter 5

Results and Discussion

5.1 Summary

This work has shown that for the treatments studied, changes in bending stiffness of the feather shafts were revealed. The changes in bending stiffness observed between the bird species and between the types of experiments were also significant. It has also been shown that it is possible to make FE-models of feather shafts that simulates the bending behavior with good agreement as compared with experiments.

Consistently, from the comparison of the results from the experiments, the Willow Warbler has lower resistance to mechanical fatigue than the Chiffchaff. Since the feathers from the Chiffchaff were older than the feathers from the Willow Warbler it strengthen these results even more. No difference could be found between the two species undergoing the UV-radiation experiment.

As for the comparison between the single and combined experiment, the combination of the UV-radiation and the mechanical wearing prevents the UV-radiation part to make the feathers stiffer as in the single experiment and the mechanical wear part gives a larger decrease of the stiffness than was observed in the single experiment.

5.2 Proposals for future work

Proposals for future work and for the continuation of the work made in this thesis are, not in order of relevance

- A study of completely fresh feathers, newly grown.
- Longer test-series and combining them with other exposures such as to bacteria.
- Make the combined test of UV-radiation and mechanical wearing simultaneously.
- A more thorough microscopical study of the feathers, investigating the different oriented keratin layers in the cortex getting a better material description and a better geometry modell.
- A more thorough analysis of the FE-model, investigating different load cases, different clamping cases and the orthotropic keratin orientation.
- An analysis of the embrittlement of the feather shaft exposed to UV-radiation by making an ultimate limit state study.

Bibliography

[1] Prys-Jones R., (1991), *The occurrence of biannual moult in passerines*, Bull. B. O. C. **111**, 150-152.

[2] Getteröns naturreservat, http://www.getteron.com, 2002-10-03.

[3] EKU Department of Biological Sciences, http://www.biology.eku.edu, 2003-03-06.

[4] Lucas A. M., Stettenheim P. R., (1972), *Avian Anatomy - Integument ,Part I*, Washington, D.C., United States of America.

[5] Bonser R. H. C., (1996), *The mechanical properties of feather keratin*, J. Zool., Lond. **239**, 477-848.

[6] Purslow P. P., Vincent J. F. V., (1978), *Mechanical properties of primary feathers from the pigeon*, J. exp. Biol. **72**, 251-260.

[7] Bonser R. H. C., Purslow P. P., (1995), *The Young's modulus of feather keratin*, J. exp. Biol. **198**, 1029-1033.

[8] Corning W. R., Biewener A. A., (1998), *In vivo strains in pigeon flight feather shafts: Implications for structural design*, J. exp. Biol. **201**, 3057-3065.

[9] Smith G. J., (1995), *Photodegradation of keratin and other structural proteins*, J. Photochem. Photobiol. **27**, 187-198.

[10] Björn L. O., Teramura A. H., (1993), *Simulation of Daylight Ultraviolet Radiation and Effects of Ozone Depletion*, Env. UV Photobiol. 41-71.

[11] Ottosen N. S., Petersson H., (1992), *Introduction to the Finite Element Method*, Prentice Hall Europe, Great Britain.

Appendices

A The original data of the collected feathers, original bending stiffness and measurements

Table A.1: *Original data of the collected feathers.*

Ringnumber	Species	Date	Age	Wing L. [mm]	Feather
RN2968	PH COL	22-May-02	20	63	HP1
RN2959	PH COL	10-May-02	3+	55	HP1
RN2963	PH COL	17-May-02	20	58	HP1
RN2964	PH COL	18-May-02	20	63	HP1
RN2965	PH COL	18-May-02	20	61	HP1
RN2966	PH COL	18-May-02	20	61	HP1
RN2962	PH COL	15-May-02	20	61	HP1
RN2951	PH COL	8-May-02	2+	63	HP1
RN2950	PH COL	6-May-02	20	58	HP1
RN2947	PH COL	8-May-02	3+	56	HP1
RN2957	PH COL	9-May-02	20	65	HP1
RN2954	PH COL	9-May-02	3+	60	HP1
RN2953	PH COL	9-May-02	20	58	HP1
RN2967	PH COL	22-May-02	20	58	HP9
RN2958	PH COL	10-May-02	20	60	HP1
BU87386	PH TRO	7-May-02	2+	70	HP1
BU87299	PH TRO	6-May-02	2+	71	HP8
BU87069	PH TRO	7-May-02	2+	69	HP1
BU87378	PH TRO	7-May-02	2+	68	HP1
BU87354	PH TRO	6-May-02	2+	72	HP1
BU87342	PH TRO	6-May-02	2+	70	HP1
BU87316	PH TRO	6-May-02	2+	63	HP1
BU87308	PH TRO	6-May-02	2+	69	HP1
BU87317	PH TRO	6-May-02	2+	71	HP1
BU87253	PH TRO	5-May-02	2+	71	HP1
BU87298	PH TRO	6-May-02	2+	72	HP1
BU87409	PH TRO	8-May-02	2+	71	HP1
BU87315	PH TRO	6-May-02	2+	64	HP1

Table A.2: *Original bending stiffness and diameter of the feathers of the Chiffchaff (PH COL).*

Test no.	Ring no.	Wing L. [mm]	Original bending stiffness	Dia. at clamp [mm]	Dia. at load [mm]
1	RN2968	63	Cancelled	0.7	0.4
2	RN2959	55	0.00095	0.5	0.3
3	RN2963	58	0.00124	0.7	0.3
4	RN2964	63	0.00255	0.75	0.4
5	RN2965	61	0.00189	0.6	0.35
6	RN2966	61	0.00192	0.6	0.35
7	RN2962	61	0.00239	0.75	0.4
8	RN2951	63	0.00237	0.75	0.4
9	RN2950	58	0.00131	0.5	0.35
10	RN2947	56	0.00132	0.65	0.4
11	RN2957	65	0.00171	0.7	0.4
12	RN2954	60	0.00146	0.7	0.4
13	RN2953	58	0.00150	0.7	0.4
14	RN2967	58	Cancelled	0.7	0.3
15	RN2958	60	Cancelled	0.7	0.35

Table A.3: *Original bending stiffness and diameter of the feathers of the Willow Warbler (PH TRO).*

Test no.	Ring no.	Wing L. [mm]	Original bending stiffness	Dia. at clamp [mm]	Dia. at load [mm]
1	BU87386	70	Cancelled	0.8	0.45
2	BU87299	71	0.00449	0.9	0.50
3	BU87069	69	0.00306	0.8	0.45
4	BU87378	68	Cancelled	0.8	0.45
5	BU87354	72	0.00331	0.8	0.45
6	BU87342	70	0.00399	0.8	0.45
7	BU87316	63	0.00279	0.75	0.40
8	BU87308	69	0.00263	0.85	0.45
9	BU87317	71	0.00334	0.8	0.45
10	BU87253	71	0.00409	0.85	0.40
11	BU87298	72	0.00544	0.85	0.40
12	BU87409	71	0.00295	0.8	0.40
13	BU87315	64	0.0024	0.75	0.40

B Bending stiffness results from the three experiments

Table B.1: *Bending stiffness results from the CUV experiment.*

Session	UV [h]	CUV1	CUV2	CUV3	CUV4	Mean
0	0	0.00255	0.0015	0.00146	0.00095	0.001205
1	24	0.00254	0.00154	0.00205	0.00124	0.001645
2	72	0.00267	0.00139	0.00228	0.00116	0.00172
3	120	0.00274	0.00173	0.00233	0.00101	0.00167
4	168	0.00278	0.00179	0.00234	0.00128	0.00181
5	216	0.00278	0.002	0.00216	0.00156	0.00186
6	264	0.00287	0.00144	0.00234	0.00169	0.002015
7	312	0.00282	0.00103	0.00185	0.00126	0.001555
8	360	0.00286	0.0012	0.00175	0.00121	0.00148
9	408	0.00284	0.00125	0.0019	0.00115	0.001525
10	456	0.00273	0.00131	0.00175	0.00112	0.001435
11	504	0.00224	0.00116	0.00177	0.00113	0.00145
12	552	0.00231	0.00099	0.00162	0.0012	0.00141
13	600	0.00243	0.00123	0.00176	0.00117	0.001465
14	648	0.00191	0.00104	0.00156	0.0011	0.00133

Table B.2: *Bending stiffness results from the TUV experiment.*

Session	UV [h]	TUV1	TUV2	TUV3	TUV4	Mean
0	0	0.00544	0.00334	0.00331	0.0024	0.0036225
1	24	0.00455	0.00345	0.00313	0.00247	0.0034
2	72	0.00488	0.00406	0.00344	0.00265	0.0037575
3	120	0.00496	0.00414	0.00356	0.00268	0.003835
4	168	0.00509	0.00422	0.00391	0.00278	0.004
5	216	0.00519	0.00412	0.00359	0.00279	0.0039225
6	264	0.00543	0.00409	0.00396	0.00275	0.0040575
7	312	0.00448	0.00395	0.0037	0.00268	0.0037025
8	360	0.00459	0.00362	0.00351	0.00275	0.0036175
9	408	0.00417	0.00342	0.00349	0.00275	0.0034575
10	456	0.00398	0.0034	0.00351	0.00262	0.0033775
11	504	0.00385	0.00308	0.00324	0.00268	0.0032125
12	552	0.00354	0.00304	0.00303	0.00245	0.003015
13	600	0.00335	0.0028	0.00275	0.0024	0.002825
14	648	0.00347	0.00267	0.00255	0.00222	0.0027275

Table B.3: *Bending stiffness results from the CMek experiment.*

Session	Strokes [n]	CMek1	CMek2	CMek3	CMek4	Mean
0	0	0.00239	0.00171	0.00192	0.00124	0.001815
1	110000	0.00246	0.00121	0.00169	0.00158	0.001735
2	198000	0.00261	0.00111	0.0016	0.00166	0.001745
3	286000	0.00249	0.00125	0.00173	0.00144	0.0017275
4	374000	0.00219	0.0008	0.00156	0.00154	0.0015225
5	462000	0.00276	0.0012	0.00155	0.00154	0.0017625
6	550000	0.00236	0.00105	0.0017	0.00158	0.0016725
7	638000	0.00222	0.00103	0.00152	0.00144	0.0015525
8	726000	0.00224	0.0012	0.0017	0.00152	0.001665
9	814000	0.00201	0.001	0.00153	0.00151	0.0015125
10	902000	0.002	0.00106	0.0014	0.0014	0.001465

Table B.4: *Bending stiffness results from the TMek experiment.*

Session	Strokes [n]	TMek1	TMek3	TMek4	Mean
0	0	0.00449	0.00306	0.00263	0.0033933
1	110000	0.00485	0.00322	0.00212	0.0033967
2	198000	0.00507	0.00357	0.00202	0.0035533
3	286000	0.00413	0.00319	0.0018	0.0030400
4	374000	0.00365	0.00228	0.00182	0.0025833
5	462000	0.00388	0.00267	0.00173	0.0027600
6	550000	0.00406	0.00264	0.0018	0.0028333
7	638000	0.00371	0.00237	0.00143	0.0025033
8	726000	0.00324	0.00226	0.00148	0.0023267
9	814000	0.00309	0.00202	0.00148	0.0021967
10	902000	0.00335	0.00212	0.00154	0.0023367

Table B.5: *Bending stiffness results from the CUM experiment.*

Session	Experiment	UV [h]	Strokes [n]	CUM1	CUM2	CUM3	CUM4	Mean
0	0	0	0	0.00237	0.00189	0.00132	0.00131	0.0017225
1	UV	24		0.00267	0.00203	0.00183	0.00105	0.001895
2	Mek		110000	0.00241	0.00194	0.00162	0.00141	0.001845
3	UV	72		0.00238	0.00193	0.00132	0.00118	0.0017025
4	Mek		198000	0.00258	0.00169	0.00143	0.00108	0.001695
5	UV	120		0.00242	0.0017	0.00133	0.00107	0.00163
6	Mek		286000	0.00198	0.00169	0.00134	0.00104	0.0015125
7	UV	168		0.00256	0.00175	0.00151	0.00099	0.0017025
8	Mek		374000	0.00254	0.00174	0.00154	0.00109	0.0017275
9	UV	216		0.00204	0.00167	0.00142	0.00098	0.0015275
10	Mek		462000	0.00197	0.00165	0.00136	0.00072	0.001425
11	UV	264		0.00215	0.00142	0.00125	0.00093	0.0014375
12	Mek		550000	0.00226	0.00134	0.00139	0.00085	0.00146
13	UV	312		0.00205	0.00156	0.00129	0.00084	0.001435
14	Mek		638000	0.00188	0.00127	0.00125	0.00089	0.0013225
15	UV	360		0.00185	0.00156	0.00127	0.00092	0.0014
16	Mek		726000	0.00182	0.00148	0.00124	0.00085	0.0013475

Table B.6: *Bending stiffness results from the TUM experiment.*

Session	Experiment	UV [h]	Strokes [n]	TUM1	TUM2	TUM3	TUM4	Mean
0	0	0	0	0.00409	0.00399	0.00295	0.00279	0.003455
1	UV	24		0.00355	0.00412	0.00278	0.003	0.0033625
2	Mek		110000	0.00385	0.00393	0.00315	0.00285	0.003445
3	UV	72		0.00375	0.00392	0.00306	0.00293	0.003415
4	Mek		198000	0.00304	0.00326	0.00276	0.00297	0.0030075
5	UV	120		0.00319	0.00358	0.00282	0.00269	0.00307
6	Mek		286000	0.0029	0.00359	0.00261	0.00227	0.0028425
7	UV	168		0.00278	0.00376	0.00282	0.00219	0.0028875
8	Mek		374000	0.00289	0.00318	0.00279	0.00195	0.0027025
9	UV	216		0.00268	0.00347	0.00279	0.00215	0.0027725
10	Mek		462000	0.00256	0.00282	0.00273	0.0021	0.0025525
11	UV	264		0.00252	0.00241	0.00234	0.00205	0.00233
12	Mek		550000	0.00229	0.002	0.0025	0.00192	0.0021775
13	UV	312		0.00234	0.00197	0.0024	0.00197	0.00217
14	Mek		638000	0.00205	0.00141	0.00188	0.00179	0.0017825
15	UV	360		0.00235	0.00175	0.00223	0.00168	0.0020025
16	Mek		726000	0.00246	0.00169	0.00231	0.00157	0.0020075

Table B.7: *Relative UV and Mek bending stiffness results from the CUM experiment.*

Session	Mean	Rel.UV	Rel.Mek
0	0.0017225	0.0017225	0.0017225
1	0.001895	0.001895	
2	0.001845		0.0016725
3	0.0017025	0.0017525	
4	0.001695		0.001665
5	0.00163	0.0016875	
6	0.0015125		0.0015475
7	0.0017025	0.0018775	
8	0.0017275		0.0015725
9	0.0015275	0.0016775	
10	0.001425		0.00147
11	0.0014375	0.00169	
12	0.00146		0.0014925
13	0.001435	0.001665	
14	0.0013225		0.00138
15	0.0014	0.0017425	
16	0.0013475		0.0013275

Table B.8: *Relative UV and Mek bending stiffness results from the TUM experiment.*

Session	Mean	Rel.UV	Rel.Mek
0	0.003455	0.003455	0.003455
1	0.0033625	0.0033625	
2	0.003445		0.0035375
3	0.003415	0.0033325	
4	0.0030075		0.00313
5	0.00307	0.003395	
6	0.0028425		0.0029025
7	0.0028875	0.00344	
8	0.0027025		0.0027175
9	0.0027725	0.00351	
10	0.0025525		0.0024975
11	0.00233	0.0032875	
12	0.0021775		0.002345
13	0.00217	0.00328	
14	0.0017825		0.0019575
15	0.0020025	0.0035	
16	0.0020075		0.0019625

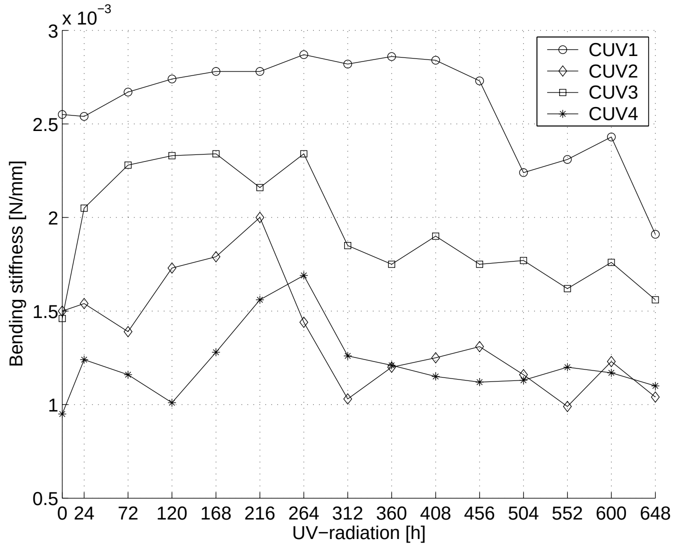

Figure B.1: *Results from bending stiffness tests after UV-radiation on the feathers of the Chiffchaff.*

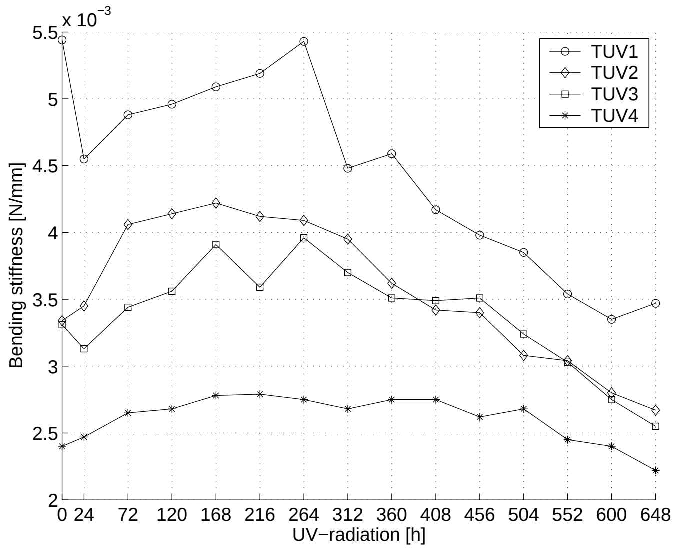

Figure B.2: *Results from bending stiffness tests after UV-radiation on the feathers of the Willow Warbler.*

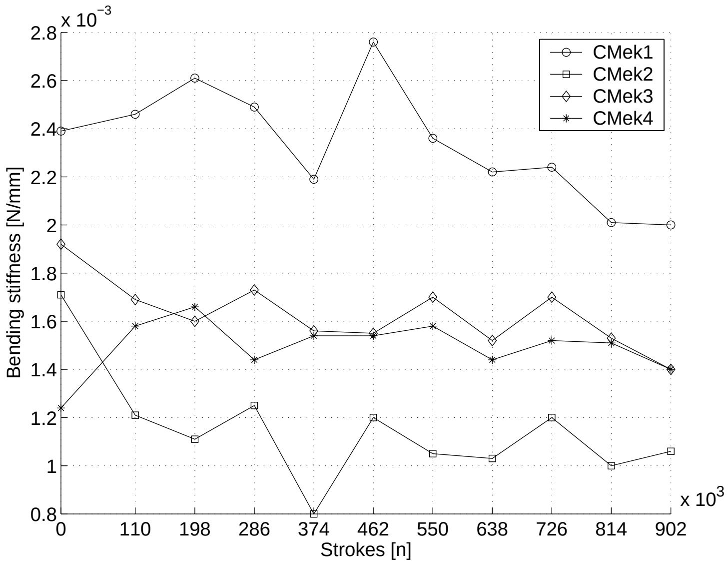

Figure B.3: *Results from bending stiffness tests after Mechanical wearing of the feathers of the Chiffchaff.*

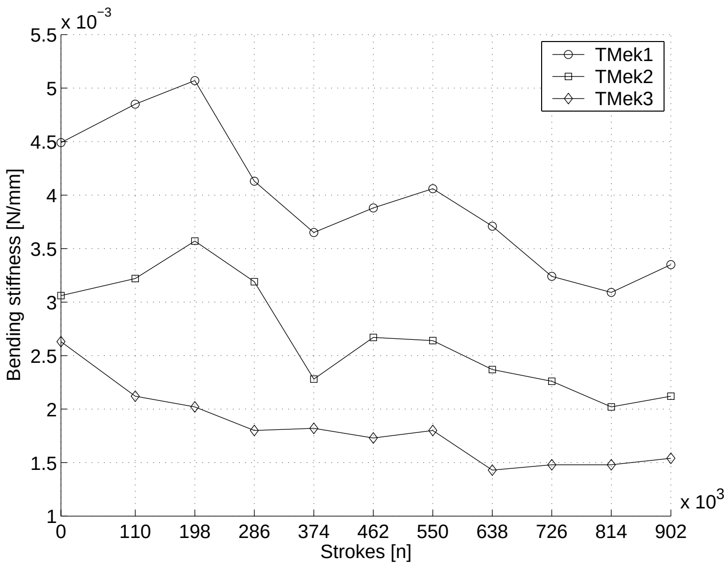

Figure B.4: *Results from bending stiffness tests after Mechanical wearing of the feathers of the Willow Warbler.*

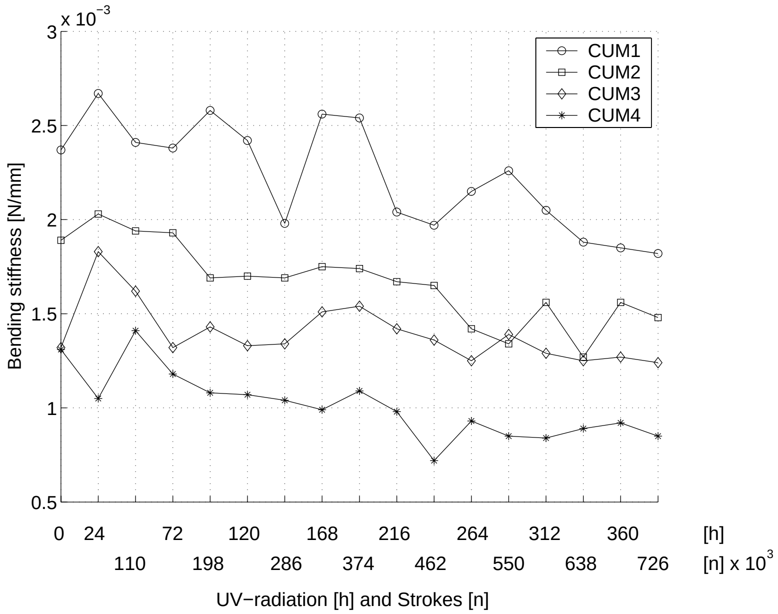

Figure B.5: *Results from bending stiffness tests after UV-radiation and Mechanical wearing of the feathers of the Chiffchaff.*

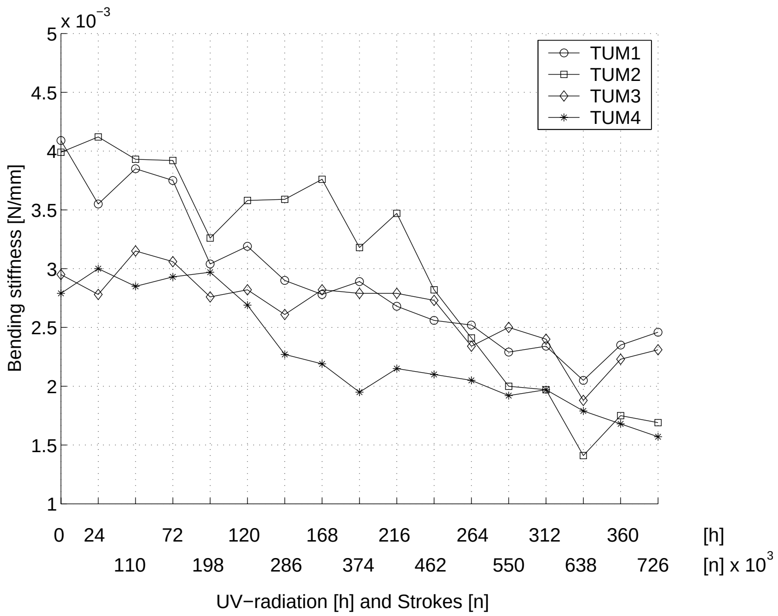

Figure B.6: *Results from bending stiffness tests after UV-radiation and Mechanical wearing of the feathers of the Willow Warbler.*

C ABAQUS Input File

```
*HEADING
**
**----------------------------------------------------------------
***                    NODES
**----------------------------------------------------------------
**
*NODE
      1,      617.798,     -702.064,        15000.
      2,      597.331,     -700.818,        15000.
      3,       576.74,     -698.317,        15000.
      .
      .
      .
  24945,      3707.07,     -2517.29,       29709.2
  24946,      3752.54,     -2543.06,       29854.7
  24947,      3798.49,     -2569.13,       29999.9
**
**----------------------------------------------------------------
***                    ELEMENTS
**----------------------------------------------------------------
**
*ELEMENT, TYPE=C3D8, ELSET=PROP1
      1,       1,       2,      33,      32,    3132,    3133,
   3164,    3163
      2,       2,       3,      34,      33,    3133,    3134,
   3165,    3164
      3,       3,       4,      35,      34,    3134,    3135,
   3166,    3165
      .
      .
      .
  11998,   21813,   21814,   12623,   12622,   24944,   24945,
  15754,   15753
  11999,   21814,   21815,   12624,   12623,   24945,   24946,
  15755,   15754
  12000,   21815,   21816,   12625,   12624,   24946,   24947,
  15756,   15755
**
**----------------------------------------------------------------
***                    MATERIAL
**----------------------------------------------------------------
**
*SOLID SECTION, ELSET=PROP1, MATERIAL=KERATIN
          1.,
**
** keratin
**
*MATERIAL, NAME=KERATIN
**
*ELASTIC, TYPE=ISO
      0.0025,         0.3
**
** E= 2.5 GPa   Young's modulus
** v= 0.3       Poisson's ratio
**
**----------------------------------------------------------------
***                    BOUNDARY CONDITIONS
**----------------------------------------------------------------
**
*BOUNDARY, OP=NEW
BOUND, 1,,          0.
BOUND, 2,,          0.
BOUND, 3,,          0.
**
```

```
**------------------------------------------------------------
***                    LOAD CASE
**------------------------------------------------------------
**
** Step  1, Default Static Step
** LoadCase, Default
**
**STEP, AMPLITUDE=RAMP, PERTURBATION
*STEP, NLGEOM
**
This load case is the default load case that always appears
**
*STATIC
 0.01,1.0,1E-8,0.1
**
**------------------------------------------------------------
***                   NODE SET
**------------------------------------------------------------
**
*NSET, NSET=BOUND, GENERATE
    3101,    3131,       1
    6232,    6262,       1
    9364,    9392,       1
   12495,   12523,       1
*NSET, NSET=LOAD
   22092,   22193,   22294,   22395,    22496
**
**------------------------------------------------------------
***                   LOAD
**------------------------------------------------------------
**
*CLOAD, OP=NEW
LOAD, 2,        -0.001    # 0-1 mN in 5 nodes => 0-5 mN
**
*DLOAD, OP=NEW
*TEMPERATURE, OP=NEW
**
**------------------------------------------------------------
***                   OUTDATA
**------------------------------------------------------------
**
*NODE PRINT, FREQ=1
U,
*NODE FILE, FREQ=1
U, RF
**
*EL PRINT, POS=INTEG, FREQ=1
S,
E,
*EL FILE, DIR=YES, POS=INTEG, FREQ=1
S,
E,
**
*EL PRINT, POS=NODES, FREQ=0
**
*EL FILE, DIR=YES, POS=NODES, FREQ=0
**
*EL PRINT, POS=CENTR, FREQ=0
**
*EL FILE, DIR=YES, POS=CENTR, FREQ=0
**
*EL PRINT, POS=AVERAGE, FREQ=0
**
*EL FILE,  POS=AVERAGE, FREQ=0
**
*MODAL PRINT, FREQ=99999
```

```
**
*MODAL FILE, FREQ=99999
**
*ENERGY PRINT, FREQ=0
**
*ENERGY FILE, FREQ=0
**
*PRINT, FREQ=1
**
*OUTPUT, HISTORY, FREQ=1
*NODE OUTPUT, NSET=LOAD
U, RF
**
*END STEP
```